Analysis of unreinforced and reinforced shallow piled embankments subject to cyclic loading

K. Aqoub[1], M. Mohamed[2]* and T. Sheehan[3]

[1] PhD research student, School of Engineering, Faculty of Engineering and Informatics, University of Bradford, Bradford, West Yorkshire, BD7 1DP, UK.

K.M.A.Aqoub@student.bradford.ac.uk

[2] Senior Lecturer, School of Engineering, Faculty of Engineering and Informatics, University of Bradford, Bradford, West Yorkshire, BD7 1DP, UK.

M.H.A.Mohamed@bradford.ac.uk

[3] Lecturer, School of Engineering, Faculty of Engineering and Informatics, University of Bradford, Bradford, West Yorkshire, BD7 1DP, UK.

T.Sheehan@bradford.ac.uk

* Corresponding author

Dr Mostafa Mohamed

Email: m.h.a.mohamed@bradford.ac.uk

Phone: +44(0) 1274 233856

Fax: +44(0) 1274 2341111

Re-submission

27 December 2018

Analysis of unreinforced and reinforced shallow piled embankments subject to cyclic loading

K. Aqoub, M. Mohamed and T. Sheehan

ABSTRACT: Reinforced piled embankment technique is becoming increasingly utilised for the construction over soft grounds due to its efficiency on reducing potential settlement, speed of construction and associated cost. Most of previous studies focused on developing understanding for the behaviour of thick embankments that are loaded with a static surcharge load. Data for the behaviour of shallow piled embankments under cyclic loadings are scarce. In this study, an experimental programme was undertaken using a fully instrumented testing rig to generate data and improve our understanding for the behaviour of unreinforced and reinforced shallow piled embankments subject to monotonic and cyclic loadings that were applied over a predetermined area of the embankment. The experimental results showed that collapse of soil arching is imminent and occurs during the first few cycles of load. However, regain of strength and recovery of the arching effect was observable during further stages of cyclic loadings due to densification of the embankment material and deformation of the soft subsoil. Inclusion of reinforcement layers was found to enhance the performance of load transfer mechanisms by concentrating stresses on pile caps. The results clearly showed a significant reduction in surface settlement, soft subsoil settlement and heaving with increasing the number of reinforcement layers.

KEYWORDS: Geosynthetics, piled embankment, arching of soil, cyclic loading, tensioned membrane, soil heaving, shallow embankment, soil reinforcement.

1 INTRODUCTION

Due to increasing world urbanisation, a high demand for the construction of infrastructures such as highway roads, bridges, railways, buildings and underground structures has been noted in recent decades. However, the existence of soft subsoil layers in several regions around the world may hinder and/or delay the construction of such an engineering project. Soft subsoil layers pose a high risk of excessive settlement and ground instability due to bearing capacity failure and potential slope movement if care is not taken. Preventative ground improvement techniques such as preloading, vertical drains and grouting can be used to minimise and/or eliminate the adverse effects on infrastructures but they are costly and time consuming. Reinforced pile embankment techniques prove to be an efficient and cost-effective solution for construction on soft clay layers in comparison to other techniques (Magnan 1994; Shen et al. 2005; Oh & Shin 2007). Coupling geosynthetics reinforcement with piles underneath soil embankments significantly enhanced the bearing capacity, reduced total and differential settlement and saved time. Reports on full-scale reinforced piled embankments are available (see for example; Almeida et al. 2007; Liu et al. 2007; Chen et al. 2008, Briançon & Simon 2012, Nunez et al. 2013 and Briançon & Simon 2017), although Love & Milligan (2003) reported concerns about inconsistency in the design approaches. Current design methods include Hewlett & Randolph (1988), Kempfert et al. (2004), BS 8006 (1995), BS 8006 -1 (2010) and Van Eekelen et al. (2013).

Loads are transferred on reinforced pile embankments through a combination of arching mechanism in the embankment fill material and membrane effect by geosynthetics layers (Villard & Giraud 1998; Villard et al. 2004). Due to the greater stiffness of the piles, shear resistance is mobilised along the soil columns above the pile caps leading to partial transfer of loads to pile caps by an arching mechanism alongside decreased pressure on the soft subsoil. The arching mechanism is well recognised since Terzaghi (1943). Aqoub et al. (2018) studied the effect of repeating sequential active and passive arching and observed that alternating the direction of movement significantly affected the magnitude of

pressure during the initial cycles irrespective of the embankment height. Inclusion of layers of geosynthetic reinforcement above the pile caps offer a substantial contribution to transferring load to piles through a membrane effect (see for example; Stewart & Filz 2005, Van Eekelen et al. 2012 a and b, Eskişar et al. 2012, Blanc et al. 2013 and Zhuang & Wang 2018). However, a deeper understanding for the precise type and contribution of different load transfer mechanisms is still required under different conditions of loading, embankment heights and reinforcement.

Several experimental, analytical and numerical investigations were conducted to study the behaviour and load transfer mechanisms in piled embankments with and without reinforcement layers (see for example; Guido et al. 1987, Jones et al. 1990, Low et al. 1994, Russell & Pierpoint 1997, Kempton et al. 1998, Han & Gabr 2002, Russell et al. 2003, Kempfert et al. 1999, Collin 2004, Jenck et al. 2009, Abusharar et al. 2009, Van Eekelen et al. 2011, 2015, Deb & Mohapatra 2013, Zhuang et al. 2014, Ariyarathne & Liyanapathirana 2014, Zhao et al. 2017, Fagundes et al. 2017 and Cui et al. 2018). The aforementioned studies reported that the behaviour and degree of soil arching is strongly dependent on many factors such as embankment height, properties of embankment soil, pile cap width, spacing between piles and tensile strength of reinforcement layers. A general consensus was reached that soil arching improves with increasing the height of embankment, pile cap width and shear strength parameters of the embankment soil. It was also noted that soil arching deteriorates with increasing the spacing between piles and the tensile stiffness of the reinforcement. The results suggested that increasing the embankment height and pile spacing and reducing the pile cap width led to higher tensile stresses in the reinforcement layers. It is worth noting that the aforementioned studies focused on the analysis of reinforced piled embankments under static loads only, which might not be representative of cases where reinforced pile embankments are subject to cyclic loading.

Limited studies have been carried out to study the behaviour of piled embankments under cyclic loading conditions, most are based on numerical analysis (Heitz et al. 2008, Han et al. 2015, Zhuang & Li 2015,

Houda et al. 2016, Lehn et al. 2016 and Zhuang & Wang 2018). It was found that arching of the soil was significantly affected by the application of cyclic loads (Heitz et al. 2008, Lehn et al. 2016 and Zhuang & Wang 2018). Heitz et al. (2008) found that inclusion of a reinforcement layer reduced the effect of vibrations significantly. The study conducted by Houda et al. (2016) on an unreinforced piled embankment suggested that the efficiency of the system increases under monotonic loads and decreases under higher cyclic loads. Despite the fact that real soil was not used in Houda et al. (2016), it was observed that about 50% of the surface settlement occurred during the first 10 cycles of loading. Notably, cyclic loads were applied over the whole area of the embankment which is not typically the case in most engineering projects e.g. highways and railways. Also, pressure and deformation on the soft subsoil were not investigated.

Zhuang & Li (2015) found numerically that traffic loads had a significant effect on piled embankment behaviour whilst the effect of the fill friction angle was very limited. Han et al. (2015), based on experimental and numerical analysis, found that arching in unreinforced embankments collapses if embankments are built with a ratio of height to clear spacing between piles of less than 3. In addition, when embankments are reinforced with a layer of reinforcement, the controlling ratio of height to clear spacing between piles drops to 1.4 indicating significant enhancement to the stability of the embankment under dynamic loading conditions by the inclusion of a reinforcement layer. However, only the effect of one layer of reinforcement was investigated. Moreover according to Zhuang & Wang (2018), it should be noted that a long period of time is required for a considerable degree of soft subsoil consolidation to occur which means that a large number of load cycles are needed to be applied in the numerical model. As a result, numerical modelling becomes time-consuming for the analysis of piled embankments under cyclic loading conditions and requires validation using experimental and/or field data. Zhuang & Wang (2018) validated their numerical results with experimental data, but the effect of number of reinforcement layers was not studied and only deep embankments were investigated.

This paper presents results from a comprehensive experimental investigation which attempted to analyse and shed light on issues related to unreinforced and reinforced shallow piled embankments that are subject to cyclic loadings e.g. traffic loads. A fully instrumented testing rig that is capable of providing measurements for pile load, load on soft subsoil, deformation measurements and tension force in reinforcement layers, was designed, manufactured and commissioned. In order to represent the effect of increasing the capacity of traffic loads during the life time of structure, three stages of cyclic loadings were applied during the test. Also, the effects of increasing the number of reinforcement layers on load transfer mechanisms, surface settlement and soft subsoil deformation were analysed and compared with those from a control test on unreinforced piled embankment under the same loading conditions. Finally, the tension of reinforcement layers was measured and analysed. The experimental results of the model tests are presented and discussed. These results provide ample data for validation of numerical models.

2 EXPERIMENTAL TESTING APPROACH

2.1 Scaling of testing rig

The dimensions of the testing rig were decided based on the scaling rules that were proposed and applied in earlier studies by Kempfert et al. (1999, 2004), Zaeske (2001), Heitz (2006) and Van Eekelen (2015) as shown in Table 1. According to Van Eekelen (2016), piles are installed at a centre-to-centre spacing less than or equal to 2.50 m and pile caps have a width greater than or equal to 15 % of the centre-to-centre pile spacing. In addition, the embankment height is at least 0.5 of the centre-to-centre pile spacing (Van Eekelen et al. 2010 and Van Eekelen 2016). In this study, the testing tank was scaled by a factor of 4.0 in comparison with field applications (the Prototype) based on Van Eekelen (2015) who used a scale factor between 1.6 and 4.50. Table 2 illustrates all scaled values in this study. Of note, the stresses in this study were selected to be the same as those in reality in order to avoid difficulties due to stress-dependent behaviour of the embankment fill material as suggested by Van Eekelen & Bezuijen

(2012) and Van Eekelen (2015). However, this may lead to overestimating the results from the model tests which should be taken in any further analytical and numerical evaluations. Careful inspection of all design methods indicated that a uniformly distributed surcharge load is used to simulate the effect of traffic load. It is worth noting that applying surcharge load over the whole area of the embankment is only valid where the embankment is of adequate height to ensure uniform distribution of load at the level of piles and soft subsoil. This is not applicable in the case of shallow embankment in which surcharge loads are applied and transferred through a relatively small zone of the embankment resulting in propagation of high stresses on the region below the loaded area. Van Eekelen & Bezuijen (2012) suggested that traffic loads can result in a pressure between 43.0 kPa and 79.0 kPa on shallow embankments with height ≤ 3 m. In addition, the average maximum applied traffic load is 62.11 kPa for 2.5 m centre-to-centre pile spacing and an embankment height of 1.0 m (Van Eekelen 2016). Traffic loads are transferred to the embankment fill through the pavement layer which can be considered as a flexible foundation or a reinforced slab depending on the materials used. The flexible foundation undergoes differential settlement while the rigid foundation undergoes uniform settlement. Due to difficulties to run tests under uniform pressure, this study was performed by applying loads on a rigid plate. A similar experimental study by Heitz et al. (2008) was carried out using a rigid loading plate. In order to explore appropriately the load transfer mechanisms of traffic loads over shallow embankment, cyclic loads are applied over a specific area of 900 mm X 1000 mm on the surface of the embankment. The cyclic loading was applied on three consecutive stages to produce mean surface pressures of 31.1 kPa, 42.2 kPa and 53.3 kPa with pressure amplitudes of 22.2, 33.3 and 44.4 kPa respectively. In each stage of loading, 1000 cycles were simulated with a frequency of 0.5 Hz. Of note, the frequency in this study was selected due to limitations with the data acquisition system.

2.2 Testing rig

A fully instrumented 2-D testing rig was designed, manufactured and commissioned to investigate the behaviour of unreinforced and reinforced pile supported embankments, although the real 3-D is more unfavourable. However, due to the complexity of the test, the model test was carried out in 2-D situation. The testing tank has internal dimensions of 1500 mm in length, 1000 mm in width and 500 mm in height and was manufactured out of wooden frames and marine plywood sheets. Figure 1 shows a schematic drawing of the testing rig with details of the measurement devices. The testing tank was placed on the top of and fastened onto four steel I-beams to ensure stability and rigidity during the application of external loads. The vertical walls of the testing tank were also stiffened by three steel square box sections as shown in Figure 1. A very smooth plastic sheet was glued to all internal surfaces of the testing tank to minimise frictional effect between soils and walls and to minimise/eliminate the loss of moisture from the soft subsoil.

Four model piles were constructed over the base of the testing tank to create three panels of soft subsoil with a clear width of 400 mm and a height of 200 mm. The rigid model piles were manufactured out of steel box sections with dimensions of 200 mm x 100 mm. It should be noted that the two intermediate model piles had a width of 100 mm whereas the two side model piles had a width of 50 mm for symmetry reasons. All model piles had a length of 1000 mm to cover the whole width of the testing tank simulating 2-D conditions as shown in Figure 1. To measure the loads on piles, two load cells were fixed on top of each intermediate model pile and placed below a thick metal plate. The model piles and load measurement equipment were then enclosed by inverted U-shaped metal sheets to protect the load cells, prevent the ingress of soil into the area around the load cells and minimise the friction between soft subsoil and piles. All model piles were fastened securely onto the I-beams underneath to prevent any potential movement during the application of surface loads. The finished top level of all four model piles was kept the same. To minimise friction with soft subsoils and protect against rusting, all model piles and the inverted U-shaped metal sheets were painted by a layer of epoxy coating. Data

186 from the load cells were utilised to determine the pressure on the pile caps at different stages of testing.
187 An additional two load cells were placed, as shown in Figure 1, at the base of the tank underneath the
188 soft subsoil in the middle panel to measure the increase in pressure on the soft subsoil due to
189 monotonic and cyclic loadings. The two load cells were covered with a rigid steel plate and a flexible seal
190 was applied on the boundary to prevent ingress of soil particles into the load cells area and to assist with
191 prevention of moisture loss as shown in Figure 1.
192 The results of Han & Gabr (2002) indicated that maximum tension occurs near the edge of the pile.
193 Therefore, it was crucial in this study that an attempt was made to capture the tension forces in the
194 reinforcement layers, in particular the bottom one. To enable this, a complex system was manufactured
195 and assembled to hold the reinforcement layer from each side and to transfer the load to external load
196 cells using a coupling mechanism. Load cells were mounted on the stiffening steel square box sections
197 that are used to strengthen the walls of the testing tank as shown in Figure 1. Two steel bars were
198 fastened to each end of reinforcement layer and can move freely with the reinforcement layer in the
199 vertical direction. The external connection was designed to be able to rotate in order to always measure
200 tangential tension forces. The utilisation of a coupling mechanism was important to ensure that
201 tangential forces were always measured. In total, eight load cells were used, two load cells in each end
202 of the reinforcement layer to measure the forces in the reinforcement layers. In order to present
203 tension force per meter, the measured loads were summed up from the two load cells of each end as
204 the width of the geosynthetic layer was 1m. Of note, no tension forces were applied on the
205 reinforcement layer at the early stage of connecting load cells, thus, load measurement in
206 reinforcement layers can be attributed exclusively to the additional self-weight of the soil and external
207 loads. Due to the limited number of load cells, tension forces could only be measured in two
208 reinforcement layers. Measured tension forces were used to determine the tensile stress on the
209 reinforcement layers.

The deformation in the lower reinforcement layer was measured at three points using three LVDTs which were connected to the bottom reinforcement layer from underneath of the testing tank as illustrated in Figure 1. Coin size aluminium plates were fastened on the reinforcement layers and connected by 3 mm diameter metal rods which were encased by a Perspex tube. Several trials were performed to ensure that the measurements taken were accurate records of the deformation of the bottom reinforcement layer. LVDTs were slightly compressed at the beginning to ensure continuous measurement of movements.

Cyclic loads were applied over an area of 900 mm x 1000 mm through a rigid plate system which was positioned at the centre of the embankment surface as shown in Figure 1. Despite the fact that loads are controlled and applied using an advanced Servo Hydraulic Actuator system installed by ServoCon Ltd, an additional load cell was placed on top of the loading area to ascertain applied loads by independent precise measurements. The actuator was controlled via computer software and could perform any loading conditions including monotonic and cyclic loads. The actuator was capable of performing controlled displacement or load tests. In this study, all tests were carried out whilst applied loads/stresses were controlled and set at predetermined values. Two LVDTs were mounted on top of the loading plate for measurement of the surface settlement of the loaded area.

All load cells and LVDTs were calibrated prior to use. Due to the number of measuring devices and huge number of data points, two data acquisition systems were utilised in this investigation to record measurements every 0.5 seconds. The accuracy of the load cells that were used for measurement of loads on piles, soft subsoils and reinforcement layers, was found to be ± 1.80 % of the measured values whereas that for measurement of the externally applied cyclic loading was ± 1.0% of the measured values. Calibration of the LVDTs indicated that deformation measurements were taken with an accuracy of ± 2.0 % of the measured values.

2.3 Material used

In this experimental study two different types of soil including soft soil and sands were utilised to develop soft subsoil and embankments respectively whereas geotextile layers were used to reinforce the embankment.

2.3.1 *Sand fill*

A typically available graded sand was used as the embankment fill material in this experimental study. The sand utilised had a range of particle sizes between 75 μm and 2360 μm. The important index properties of the utilised sand are summarized in Table 3. According to BS EN ISO 14688-2:2004, the sand soil was classified as even-graded coarse sand with silt and fine gravel.

2.3.2 *Soft subsoil*

In this study, a real soft subsoil was prepared and used as a sub-grade soil in all experiments. Three different types of soil namely coarse sand (CS), fine sand (FS) and pure clay powder (C), were mixed with proportions of 50 %, 25 % and 25 % respectively to create the soft subsoil. Maximum dry density and moisture water content were determined from results of standard Proctor test which are shown in Figure 2. Specimens were then prepared at maximum dry density and corresponding moisture content for measurement of the elastic modulus using Unconfined compression test. The measured elastic modulus of the proposed soft soil was found to be 16 MPa which was considered to be very high for the purpose of the tests. In order to reduce the elastic modulus, specimens were prepared in the wet-side of the compaction curve by incrementally increasing the moisture content up to 22% and tested in triaxial testing machine under Unconsolidated – Undrained condition. The elastic modulus of specimens that were compacted at a dry unit weight of 15.95 kN/m^3 and moisture content of 22 % was found to be 425 kPa which was quite low to represent weak soft subsoil. The important index properties of the selected mixture are summarized in Table 4 according to BS 5930:1999 and BS EN ISO 14688-1:20. The prepared soft subsoil was classified as clay soil with low plasticity. It should be noted that pore water pressure was

not measured in this testing programme since the time required for consolidation is much longer than the time needed to apply all three stages of cyclic load.

2.3.3 *Reinforcement*

Careful consideration was given to the selection of reinforcement material so that a realistic behaviour for reinforced piled embankments could be simulated and assessed. As explained in section 2.1, the whole testing setup was scaled down by a factor of 4. As a result, a reinforcement material with a low tensile strength of 9 kN/m' was required for this study. Several reinforcement materials have been considered including geotextile and geogrid sheets. However, geogrids were excluded as available products have a much higher tensile strength than required and since the outcomes of Van Eekelen et al. (2012) suggested that there is no major difference in the interaction between geotextile and geogrids in piled embankment. Geotextile reinforcement materials were tested for use in this study. However, geogrids are commonly used on reinforced piled embankments. A wide-width tensile test was carried out the in the lab according to BS EN ISO 10319:2015 on specimens of geotextile materials. Figure 3 shows the attained tensile stress against tensile strain results for the selected woven Polypropylene (PP) geotextile material. It can be seen that the maximum tensile strength of reinforcement materials was found to be 12.50 KN/m' which was recorded to occur at a strain of 11.0 %. The reinforcement material loses its strength post peak value. However, at 5% strain, the material can sustain a stress of 5.8 kN/m' which is well below the value required by scaling down the whole testing rig. In addition, nearly elastic behaviour was noted in the first 2% strain which is expected to occur in this kind of reinforcement material. Layers of woven PP geotextile with dimensions of 1400 mm in length and 1000 mm in width were used as reinforcement materials.

2.4 Testing setup, procedure and programme

Prior to the onset of the experimental programme, the testing tank was positioned in the central area of the loading frames so as to be centred with the actuator. Furthermore, the testing tank was also levelled to be precisely horizontal so that it was perpendicular to the vertical axis of the actuator.

The soft subsoil was prepared by mixing specific amounts of CS, FS and C and adding a predetermined quantity of water in a large mechanical mixer to ensure achieving a uniform mixture. In total, around 400 kg of soft soil was prepared and stored for re-use in all tests. The soft soil was placed and compacted manually in layers of 50 mm to fill in the space between the model piles. Once the soft soil was levelled off with the model piles, the surface of soft soil was covered by a dump proof sheet and surcharge pressure of 2.0 kPa was applied for 24 hours to ensure reaching; (1) a uniform distribution of water and (2) a pre-set dry unit weight which was determined based on the measurements taken by the load cells that were installed underneath the base of the soft subsoil. After the elapse of the 24 hr period, the surcharge load and dump proof sheet were removed and any subsidence on the surface of the soft subsoil was re-filled by the addition of the same soft soil. Ultimately, the surface of the soft subsoil was levelled off insuring that it coincided with the top level of the piles. Readings from the load cells underneath the soft subsoil in middle panel were taken to record the total weight of wet soft subsoil in each test. In addition, three specimens were collected for the determination of actual water content. The dry unit weight was then determined using the measured wet weight of the soft subsoil and the measured water content.

In order to prepare the embankment with the same dry unit weight, a sand raining technique was employed in this testing programme by which sand was poured through a perforated metal sheet that was placed at the top of the testing tank. A trial test was conducted in which 20 samples were collected from different heights and locations within the embankment for the determination of the dry unit weight. It was found that the average dry unit weight of the sand was 16.80 ± 0.05 kN/m^3. The achieved dry unit weight was almost 94% of the maximum dry unit weight determined from the standard Proctor

304 test. According to Das (2010), the achievable dry density in engineering practice is required to be
305 between 90% and 105%. Thus, the achieved dry unit weight of the embankment fill was considered to
306 be acceptable.
307 In this study, around 520 kg of sand was poured into the testing tank through the raining box. For
308 unreinforced embankments, continuous raining of sand was maintained until reaching the required
309 height. Then the surface of the sand bed was levelled off to avoid any discrepancy in the initial
310 overburden pressure and detrimental effects on the loading area. Whereas, in the case of inclusion of
311 reinforcement layers, sand raining was interrupted to allow the insertion of reinforcement layers at
312 predetermined heights according to the testing programme. The bottom layer was always placed on top
313 of a sand bed with a thickness of 25 mm to prevent damaging of the reinforcement layer by the sharp
314 edge of the model piles. Subsequently, the two ends of the reinforcement layer were fastened to the
315 tension measurement mechanism and LVDTs were connected from underneath the testing tank. Then
316 sand raining was resumed to form the embankment until reaching the required level. In the case of
317 inclusion of additional layers of reinforcement, sand raining was temporarily ceased to enable the
318 installation of reinforcement layers at particular levels. Of note, the sand surface was always levelled off
319 prior to the placement of reinforcement layers which were inserted at a spacing of 50 mm.
320 Once the top level of the embankment was levelled off, this denotes the completion of stage 0 and
321 records of load cells were taken as shown in Figure 4. The loading plate was placed on the central area
322 of the testing tank. Two LVDTs were securely mounted on top of the loading plate to measure
323 settlement as shown in Figure 1. Then the Servo Hydraulic Actuator was moved down slowly until it
324 became in contact with the loading plate. Stage I of loading which is monotonic loading was initiated by
325 gradually increasing the applied load up to 28 KN at a rate of 0.42 kN/sec. The load was maintained
326 constant for 200 s. Then three stages of cyclic loading with different mean loads and amplitudes were
327 performed with a constant frequency of 0.5 Hz. The cyclic loading in stages II, III and IV were (8-48 kN),

(8-68 kN) and (8-88 kN) which are equivalent to the application of surface pressures of (8.9-53.3 kPa), (8.9-75.6 kPa) and (8.9-97.8 kPa) respectively. The amplitude of the applied load was increased with the stage to simulate, to a great extent, the on-off nature of different cyclic loadings. Due to limitations with the data acquisition systems, data were recorded every 0.5 s so that four readings could be taken every load cycle. The number of cycles in all three stages of cyclic loading was kept at 1000 cycles. After the 3000 cycles were completed, the loading in stage V was reduced gradually at a rate of 0.42 kN/sec until complete unloading. Upon removal of the loading plate, the soil surface was scanned accurately to determine surface profile in particular areas of settlement and heave. Furthermore, the surface profile of the soft subsoil was accurately scanned after the removal of the embankment fill material. Finally, specimens of clay soil and sand soil were taken for determination of water content. In this study, four experiments were performed in order for a deeper understanding of the behaviour of shallow unreinforced and reinforced piled embankment under cyclic loading conditions to be acquired. All tests were undertaken whilst the thicknesses of the soft subsoil bed and sand soil bed were kept at 200 mm, but the number of reinforcement layers was varied from zero to three layers.

3 RESULTS AND DISCUSSIONS

In this section, the results attained for loads and deformations were presented and analysed. All experiments were conducted under 5 stages of loading namely; self-weight (stage 0), monotonic load (stage I), cyclic loading 1 (stage II), cyclic loading 2 (stage III), cyclic loading 3 (stage IV) and unloading stage (stage V) as shown in Figure 4. The effect of number of reinforcement layers on the behaviour of soil arching, settlements and heaving were discussed and compared here after. Of note, (1) all measured loads on piles and soft subsoil are converted into pressure for the sake of comparison and to aid the discussion, and (2) due to the huge number of data points, data points presented in figures represent the average of measured maximum and minimum values of five consecutive cycles. It should also be noted that some discrepancies were observed in the measured data. The pressure difference on

the two piles did not exceed 6% whist the discrepancy in the reinforcement tension force from the left- and right-hand side load cells was less than 7 %. The difference in measured surface settlement by the two LVDTs was less than 4%. It should also be noted that the results presented hereafter represent measured values from the model scale tests without any scaling corrections.

3.1 Analysis of unreinforced and reinforced embankment

Figure 5 presents the variations of maximum pressure on piles and soft subsoil versus time during different stages of loading on 200 mm unreinforced embankment. Initially, under the self-weight of the embankment (stage 0), it can be seen that the measured pressure on the soft subsoil was nearly the same as the pressure on the piles. These values are corresponding to the weight of embankment soil which indicated that no active arching was formed. This can be attributable to the embankment material being at rest conditions. However, when monotonic load was initiated (stage I), the pressure on the soft subsoil started to increase but at a slower rate. Significant increase on the pressure was recorded to occur on the piles. For a surface pressure of 31 kPa, the pressure on the pile caps was measured to be about 68 kPa and that on the soft subsoil was about 17 kPa which means that soil arching was developed and caused significant transfer of loads to piles. This is in agreement with Girout et al. (2018) who found that the transferring of load to the pile was increased when the surcharge external load was applied compared with the case without applying surcharge load (overburden pressure).

During stage II, cyclic load was applied with pressure between (8.9 kPa and 53.2 kPa). At the maximum applied load, it can be seen from Figure 5 that a remarkable drop in pressure on the pile caps occurred accompanied with a substantial pressure increase on the soft subsoil. This indicated the collapse of the formed arch in the embankment soil during the initial cycles of load. The pressure on the pile cap was decreased by 15% from 96 kPa to about 82 kPa over the first 16 cycles. This is attributable to the loss in mobilised shear resistance along the vertical soil columns above pile caps by cyclic loads causing significant damage to the formed soil arching which is consistent with earlier findings by Heitz et al.

(2008), Zhuang & Wang (2018) and Wang et al. (2018). However, with increasing the number of load cycles, the rate of reduction in arching resistance decreased, thus after 400 cycles, the pressure on pile cap was decreased by 25 % from 82 kPa to about 72 kPa. Then there was hardly any further reduction in the pressure on the pile until the end of this stage.

Despite the collapse of soil arching during the first stage of cyclic loading, entirely the opposite behaviour was noted during subsequent stages of cyclic loads (stages III and IV) in which the higher surface cyclic loading was applied. The results confirmed that most of the load was transferred to the piles causing a significant pressure increase on pile caps alongside a minor increase on the soft subsoil. From Figure 5, one could notice that pressure on the pile caps increased up to 122 and 176 kPa for surface cyclic pressures of 75.6 and 97.8 kPa respectively. Furthermore, it can be noticed that most of the load transfer occurred during the first 200 cycles followed with a gradual but very slight change until the end of each stage (1000 cycles). This could be attributed to the reinstatement of soil arching due to; (1) increased dry unit weight of the embankment fill and (2) deformation of the soft subsoil. Van Eekelen (2015) and Bhasi & Rajagopal (2015) found that consolidation of soft subsoil improves the arching in the embankment fill. In these experiments soft subsoil deformation was observed under the increased pressure by external cyclic loading. Improved shear strength of the embankment material was also imminent due to increased dry unit weight under the effect of load cycles. This could be due to densification of the embankment fill material by the act of dynamic compaction caused by the effect of cyclic loading which is consistent with recent observations made by Elshesheny et al. (2018) when cyclic loadings were applied over a small area in unreinforced and reinforced sand beds. Data taken for deformation of the embankment surface and soft subsoil were used to estimate the change in volume of the embankment fill material. Since the weight of sand used to build the embankment was measured, the dry unit weight could then be estimated. Figure 6 shows the estimated dry unit weight of the embankment material during the three stages of cyclic loading. The results show a degree of

400 improvement in the dry unit weight of the embankment in particular during the early period of
401 application of cyclic loading. As a result, some improvement in the shear strength of the embankment
402 materials leading to recovery of the arching effect would be experienced which resulted in the transfer
403 of loads to piles in subsequent stages of load. The results in this study suggest that both increase in dry
404 unit weight and deformation in soft subsoil caused significant improvement to particle interlocking and
405 development of strong arching in the embankment fill material which in turn led to significant transfer
406 of pressure on to pile caps.
407 Figure 5 also shows the variations of minimum pressure on piles and soft subsoil versus time during
408 different stages of loading. During stage II, a slight reduction in the pressure on the pile accompanied
409 with a slight increase in soft subsoil was observed during the initial cycles and then the pressure
410 remained constant until the end of the cyclic loading stage. The pressure on the pile cap was decreased
411 by 13 % from 30 kPa to about 26 kPa over the first 20 cycles. During stages III and IV, the pressure on
412 the piles and soft subsoil was slightly increased although the minimum applied load was kept the same
413 during each loading stage.as shown in Figure 5. In addition, from the close-up graphs in Figure 5, it can
414 be clearly seen that most of the cyclic load was taken by piles and increased with increasing the applied
415 pressure while the amplitude of pressure on the soft subsoil was quite small during all cyclic loading
416 stages in comparison with that recorded on piles. The measured amplitude of pressure on the piles
417 during the first stage of loading was varied between 28 kPa and 82 kPa while the measured amplitude of
418 pressure on the soft subsoil during the first stage of loading was varied between 20 kPa and 28kPa.
419 During the third stage of cyclic loading the measured amplitude of pressure on the piles during was
420 varied between 43 kPa and 196 kPa while the measured amplitude of pressure on the soft subsoil was
421 varied between 20 kPa and 35 kPa.
422 Inclusion of one, two and three reinforcement layers at predetermined locations was examined to
423 evaluate the effects of reinforcement on the load transfer mechanisms within the embankment fill

material, particularly to illustrate how the reinforced embankment system responds to external cyclic loads. Figures 7, 8 and 9 show the effect of number of reinforcement layers on measured maximum pressure on pile caps and soft subsoil during all stages of loading. During stage 0 and I (overburden and monotonic loading stages), it can be seen that increasing the number of reinforcement layers caused a slight increase in pressure measured at the pile caps accompanied by a slight reduction in the pressure on the soft subsoil. With the inclusion of three layers of reinforcement, a 15% pressure increase on the pile caps was recorded due to the self-weight of the embankment. During the application of monotonic loading, a slight improvement to the load transfer mechanism was observed with the inclusion of two and three layers of reinforcement. The pressure on the pile cap was measured to be 74 and 78 kPa for embankments reinforced with two and three layers of reinforcement giving pressure increases of 9 and 15 %. No effect was observed with the inclusion of one layer of reinforcement. This is due to the mobilised frictional resistance not being high enough to develop tension membrane effect.

Nevertheless, a major benefit for the inclusion of reinforcement could be observed once cyclic load was applied after the monotonic load in stage II. Shortly after the onset of cyclic loading, the pressure on the pile caps was recorded to be 98, 120 and 136 kPa for embankments reinforced with one, two and three layers of reinforcement. This means that enhanced load transfer mechanisms within the embankment were experienced during cyclic loading with increasing the number of reinforcement layers leading to a higher pressure on the pile caps. With the inclusion of one reinforcement layer, it is likely that the tension membrane effect which is deformation dependant, is dominant causing increased transfer of loads to the pile caps. With the addition of more reinforcement layers, the stiffness of reinforcement and stiffness of the reinforced embankment increases causing the reinforced embankment to behave as a heavily reinforced slab which is in agreement with previous observations by Mohamed (2010). Hence, an enhanced response to cyclic load was observed during various stages of loading on reinforced embankments. It should be noted that increasing the number of reinforcement layers without changing

448 the summed stiffness would show negligible difference in the behaviour of the reinforced embankment
449 (Heitz 2006 and Ariyarathne & Liyanapathirana, 2014). Inclusion of reinforcement layers lessened the
450 immediate damage to the arch formed in the embankment material which was observed in Fig. 5 and
451 the subsequently gradual decline in transferred pile cap pressure in comparison with the unreinforced
452 soil embankment. Consequently, the degree of deterioration of transferred load to pile caps which can
453 be assessed by the loss of resistance over prolonged cycles, reduced with increasing the number of
454 reinforcement layers. For the embankment with one layer of reinforcement, the measured pressure on
455 the pile caps went down to 80 KN/m^2 at the end of stage II after 1000 cycles as shown in Figure 7.
456 Increasing the number of reinforcement layers increased the stability of the load transfer mechanisms.
457 Comparing Figures 7-9 indicates that the drop in pressure on the pile caps over the 1000 cycles of stage
458 III of loading was reduced with increasing the number of reinforcement layers. When three layers of
459 reinforcement were placed, the pressure on the pile caps decreased to 128 KN/m^2 at the end of stage II
460 of loading.
461 Similar load transfer behaviour was observed with increasing the applied cyclic loading (stages III and IV)
462 but even with an enhanced level of interaction and resistance. The results in Figures 7-9 illustrated that
463 there was a minor increase in the pressure transferred to the soft subsoil whereas most of the pressure
464 increase was taken up by the piles over the first 50~60 cycles. Furthermore, the load transfer response
465 was different to stage II, a gradual increase in pressure on the pile caps was noticeable in most cases of
466 inclusion of reinforcement layers and cyclic loads. This could be attributable to enhanced interaction
467 between reinforcement layers and surrounding embankment material due to densification of
468 embankment material and deformation of the underlying soft subsoil.
469 Also, Figures 7, 8 and 9 show minimum pressure on the piles and soft subsoil during the cyclic loading
470 stages (stages II, III and IV). It can be noted that the minimum pressure on the piles increased whilst the
471 pressure on soft subsoil decreased with increasing number of reinforcement layers during all stages of

cyclic loading. For a reinforced piled embankment with three layers of reinforcement, the pressure on the pile cap increased from 33 kPa to 46, 50 and 53 kPa at the end of stage II, III and IV respectively as shown in Figure 9.

Careful inspection of pressure data on pile caps during stages III and IV in Figures 5, 7, 8 and 9 illustrates that the maximum pressure on the central piles increased significantly with increasing the number of reinforcement layers. The maximum measured pressure on the pile caps was 196, 220, 231 and 257 kPa from tests with zero, one, two and three layers of reinforcement. Since, the applied surface pressure was precisely similar in all experiments, the results therefore suggest that inclusion of the reinforcement layers enhanced the transfer of load to piles. The results also illustrated that under prolonged cycles, the pressure on the soft subsoil has experienced a very minor reduction rather than an increase which could be attributed to the effect of the soft subsoil deformation on load transfer mechanisms. It is clear that complex interactions occur on the shallow reinforced embankment subject to cyclic loading due to changes in dry unit weight of the embankment, deformation of the underlying soft subsoil and interactions between the reinforcement layer and adjacent soils. The qualitative analysis of the data for dry unit weight implies that a good degree of densification to the embankment material occurs during the initial stage of cyclic load and reduces with further stages of loading and with the inclusion of reinforcement layers. Thus, the initially determined angle of friction for the embankment material and interface characteristics between the reinforcement material and adjacent soil may improve with prolonged cycles of external loading. The interface is characterised between reinforcement layers and adjacent soils and is a function of the normal stress which in the case of shallow embankments subject to traffic loads varies substantially along the perpendicular length of the reinforcement. Thus, variation in the friction resistance is imminent on the reinforcement layers. The relative contribution of different load transfer mechanisms is therefore dependant on fill material shear strength, frictional resistance and subsidence on underlying soft subsoil alongside with other factors e.g. pile spacing and thickness of

496 embankment. However, the contribution of each mechanism cannot easily be identified and/or
497 quantified.
498 In order to aid the discussion, the efficiency of load transfer to the piles and stress concentration ratio
499 were determined. Efficiency is defined as the ratio of the embankment load transferred to pile in kN to
500 the total load of the embankment in kN (Abusharar et al. 2009). However, this definition for the
501 efficiency was proposed and developed for a uniformly distributed surcharge pressure over the whole
502 surface area of the embankment. Calculations based on this definition are therefore no longer valid for
503 assessing the efficiency of load transfer mechanisms due to the nature of applied loads e.g. traffic loads
504 or train tracks for which the external load would be applied over a particular area of the embankment
505 surface. Consequently, the pressure on pile caps would be different and directly related to the proximity
506 of each pile cap to the loaded surface area. This issue is exacerbated where loads are applied on shallow
507 embankments in which stresses would be very concentrated on a relatively small zone of the
508 embankment that is beneath the loaded area. To overcome these difficulties with the calculation of
509 efficiency, it was proposed to determine the efficiency based on measured data for transferred load to
510 central piles and central soft subsoil panel. Thus, the efficiency is determined as the ratio of the
511 embankment load transferred to pile in kN to the total load on pile and soft subsoil in kN. These values
512 would represent the minimum efficiency (worst case scenario). Figure 10 shows the measured variations
513 on the efficiency (E) of load transfer to piles versus the number of cycles of unreinforced and reinforced
514 embankments using Equation 1 whereas Figure 11 illustrates the stress concentration ratio (SCR)
515 between piles and soft subsoil in the central region underneath the loaded area based on Equation 2.

516 $$\mathrm{E}\ (\%) = \frac{a\sigma_p}{a\sigma_p + s'\sigma_s} \times 100 \quad (1)$$

517 $$\mathrm{SCR} = \frac{\sigma_p}{\sigma_s} \quad (2)$$

518 Where, E is load transfer efficiency in %, a is the width of central piles in m, σ_p is the measured
519 pressure on piles in kN/m^2, s' is pile clear spacing in m, σ_s is the measured pressure on soft subsoil in
520 kN/m^2, and SCR is stress concentration ratio.

521 It is clear that the load transfer efficiency (E) and stress concentration ratio (SCR) improved significantly
522 with the addition of reinforcement layers and slightly with further increases in the applied cyclic loads.
523 In particular, inclusion of reinforcement layers reduced the expected loss of efficiency with prolonged
524 cycles and under higher cyclic loading. It should be noted that the determined efficiency represents
525 lower boundary values and other piles that are not in close proximity would be expected to retain higher
526 efficiency. This is due to the nature of the external load e.g. traffic load that was applied over a specific
527 area of the embankment and the fact that the embankment had a shallow thickness. Although the stress
528 concentration ratio was reasonably high as can be seen in Figure 11, this was not reflected in the

529 determined pile efficiency in the central region due to; (1) the characteristics of the piled reinforced
530 embankment in the experiment, (2) the nature of the applied dynamic load, (3) the effect of applying
531 loads over a rigid plate and (4), the application of surcharge load over a particular area of the
532 embankment.

533 In this study, experiments were conducted on piled reinforced embankments with a ratio of the pile cap
534 width to centre-to-centre pile spacing of 5 and a ratio of embankment height to pile spacing of 0.5. This
535 implies that the tested system for shallow embankments on widely spaced piles would result in lower
536 stress concentration and less arching action. Abushara et al. (2009) found that the efficiency was
537 decreased from 60% to 40% by increasing the pile width to centre to centre pile spacing ratio from 1:2.5
538 to 1:4 whilst keeping the ratio of unreinforced embankment height to pile spacing at 1.0. It is well
539 documented that dynamic loads affect the strength of soil and cause fatigue to the reinforcement (see
540 for example; Zanzinger et al. 2010). It can be seen from Figure 10 that starting cyclic loading caused a

significant loss in the efficiency of the unreinforced embankment. Inclusion of reinforcement layers mitigated the loss of efficiency so that with three of layers of reinforcement, efficiency was maintained at the same level irrespective of the applied load. The results confirms that addition of more than one layer of reinforcement enhances the performance of piled reinforced embankments subject to cyclic loads.

It is also noted that differences appeared on the stress distribution below a load area based on the rigidity of the plate. In the case of rigid plate/footing above granular material as in this study, the maximum pressure occurred beneath the centre of the loaded area (Aziz 2000). Thus, even with a load spread angle, the maximum pressure still occurred in the central area of the embankment, leading to pressure concentration on the central panel of the soft subsoil and piles and leading to lower efficiency. Finally, applying loads over a particular area on shallow embankments needs serious consideration due to the concentration of stress on a small region of the embankment. As a result, the variation of shear stress along the reinforcement layer is likely to occur and may lead to a different extension of the reinforcement material.

3.2 Tension force in and deformation of reinforcement layers

Measurements of the forces generated on the reinforcement layers were taken by four load cells attached to both ends of each reinforcement layer. Of note, only the forces in two of the reinforcement layers could be measured due to the limited availability of load cells. In addition, tension force was measured at the two ends of each reinforcement layer. Of note; the maximum tension force would occur on the edge of the central piles underneath the loaded area. Figure 12 shows the variation in the tension forces during the three stages of cyclic loading on different embankments.

It can be seen that the reinforcement layers responded instantaneously to cyclic loads with the greatest tension force occurring in the embankment system with one reinforcement layer. Upon the application of cyclic loads (stage II), an immediate increase in the tension force was measured, as shown in Figure

12. The tension force in the reinforcement layers was directly related to the stage of the applied cyclic load. With increasing the number of reinforcement layers, a reduction in the tension force in the reinforcement layers was noticeable. However, the results indicated that the maximum tension forces always occur in the bottom layer. This is in agreement with Heitz et al. (2008) and Van Eekelen (2015) who found that highest strain was recorded in the bottom layer which corresponds to higher tensile stresses. Also, it can be noted that the measured tension decreased slightly during the second and third stages of cyclic loading (stages III and IV) which could be attributed to creep behaviour. Creep in reinforcement layers occurs when the reinforcement layer is under applied loads for long period of time (see for example; Ariyarathne et al. 2013) or under cyclic loadings (see for example; Kongkitkul et al. 2004). Although in this study, the time of applying loads was not long, creep in the form of residual deformation may occur and reduce the tension in reinforcement layers due to the nature of cyclic loading as suggested by Kongkitkul et al. (2004).

Figure 13 presents the maximum deformation patterns at three points on the bottom layer of reinforcement. Points 1, 2 and 3 are located in the centre of the central panel, near the edge of the central panel and the centre point of the adjacent panel as shown in Figure 1. Of note, it can be observed that a slight difference in the deformation of Points 1 and 2 of less than 2mm existed which can be attributed to the effect of boundary conditions. The results show clearly that the deformation of the reinforcement layer is at a maximum value in the central panel which reflects higher pressure due to the surface loads. From Figure 13, it can also be seen that with the inclusion of more reinforcement layers (two or three layers), a substantial reduction in the deformation of the bottom layer can be achieved, not only in the central panel but also in the neighbouring panels. By careful inspection of data in Figures 12-13, it is clear that the results of deformation and tension forces in the reinforcement layers are in agreement. In addition, the captured patterns for deformation and tension forces show similarities in the reaction towards the applied cyclic loads during the three stages of load increase. The

589 results show that the deformation of Point 3 decreases with the increase in the number of
590 reinforcement layers and is much less than that measured for Point 1. This confirms that less pressure
591 was transferred to the two neighbouring soft subsoil panels with increasing the number of layers. In
592 other words, stresses were intensified within the central region with increasing the number of
593 reinforcement layers due to increased stiffness of the reinforced zone as it was evident from increased
594 pressure on the central piles. This means that for a single layer of reinforcement, the tension membrane
595 would be dominant in transferring the loads whilst with increasing the number of reinforcement layers,
596 the reinforced zone works as a stiffened platform to transfer the loads to the piles. These results are in
597 good agreement with the outcomes of the numerical analysis by Ariyarathne & Liyanapathirana, (2014)
598 which found that the multi-layer reinforced system works as a stiffened platform while an embankment
599 system with a single layer of reinforcement works as a tensioned membrane.

600 **3.3 Settlements analysis**

601 Figure 14 presents the measured maximum settlement of the loaded area from tests on unreinforced
602 and reinforced embankments versus the number of cycles. It can be seen that during stages 0 and I
603 (static loads), the measured settlement of the loaded area is negligible in comparison with the
604 settlement of the subsequent cyclic loading stages. Non-linear relationships for the measured surface
605 settlement were very noticeable during the 1000 cycles of each stage of cyclic loading. It is clear that
606 settlement decay occurred with further cycles. Increasing the average pressure and amplitude resulted
607 in increasing the settlement but at a lower rate. This could be attributed to the densification of the
608 embankment material as illustrated in Figure 3. The results illustrated that in the case of unreinforced
609 embankments, the surface settlement was about 17.50 mm by the end of stage II and increased to 24.50
610 mm and 32.50 mm by the end of stages III and IV respectively as shown in Figure 14. However, inclusion
611 of reinforcement layers caused a significant reduction to the observed surface settlement of the
612 embankment as well as causing a further increase in the decay of settlement during stages II-IV. Results

613 of a test on a reinforced embankment with one layer showed a decreased settlement to 15.8, 21.8 and
614 26.8 mm at the end of stages II, III and IV respectively giving around an 18% reduction in the total
615 settlement. Measured final settlements at the end of stage IV were almost 26.8, 22.8 and 19.1 mm for
616 embankments reinforced with one, two and three layers of reinforcement respectively. Inspection of
617 the results indicated that almost half of the total settlement occurred during stage II (first stage of cyclic
618 loading) although the applied cyclic load during this stage was the lowest. This implied that significant
619 rearrangement of soil particles occurred under the first stages of cyclic loading which in turn led to
620 substantial densification of the embankment fill material as well as settlement of the underlying soft
621 clay. Consequently, interaction between reinforcement layers and adjacent soils would improve which
622 in turn contributed to the reduction in settlement in subsequent stages. Results of Houda et al (2016)
623 on an unreinforced embankment indicated that about 50% of the surface settlement occurred during
624 the first 10 cycles of 50 cycles. In addition, the rate of reduction in void ratio of embankment material
625 decreased with the number of cycles, which improved the arching effect.
626 Figure 15 shows the deformed shape of the embankment surface after the removal of the loading plate
627 for unreinforced and reinforced embankments. It is clear that soil heaves on both sides in all tests but
628 reduces significantly with the inclusion of reinforcement layers. Measured heave reduced from 29mm to
629 1mm for unreinforced embankments and embankment reinforced with three layers of reinforcement
630 respectively. The results therefore suggest that serious considerations need to be given to construction
631 of unreinforced or lightly reinforced shallow embankments. Increasing the number of reinforcement
632 layers clearly impacted positively on the experienced embankment soil heave due to the development
633 of shear stresses along the reinforcement layers leading to increased confinement of the embankment
634 material (see for example; Zhang et al., 2006 and Latha & Murthy, 2006). In addition, inclusion of
635 reinforcement layers enhancing the load transfer mechanisms to pile caps and potentially reduced
636 deformation of the underlying soft subsoil and embankment soil heave. The results of Rowe & Li (1999)

637 suggested that increasing reinforcement stiffness caused a significant reduction in maximum vertical
638 settlement and heave.
639 Figure 16 shows the scanned deformation of the soft subsoil surface upon the completion of tests and
640 removal of embankment materials. Distinct patterns of deformation formed in the central panel and the
641 two neighbouring panels of soft subsoil. The central panel that was centred with the loading area
642 showed a major compression and subsidence with the maximum values recorded on the centreline. The
643 results show clearly that a significant reduction in the subsidence of the soft subsoil in the central panel
644 was observed with increasing the number of reinforcement layers. Remarkably, the two neighbouring
645 soft subsoil panels showed a mix of subsidence and heave. This could be attributed to the non-uniform
646 increase of pressure due to external loading which gave indications of the lateral extent of the pressure
647 increase. It was noticed the heave on the soft subsoil was always less than the subsidence. The surface
648 deformation of the soft subsoil was alleviated with the inclusion of reinforcement layers as can be seen
649 in Figure 16. In addition, it can be seen that punching mechanism was occurred in the case of zero
650 reinforcement layer at the boundary of middle piles. Also, it can be noted that some degree of
651 settlement at the boundary of the pile in reinforced embankments was observed as shown in Figure 16.
652 Of note, image analysis was performed in order to estimate the deformation at the piles boundary.

653 **4 CONCLUSIONS**

654 An experimental programme was undertaken using a fully instrumented testing rig to assess the
655 behaviour of unreinforced and reinforced shallow piled embankments under monotonic as well as cyclic
656 loadings. Soft clay material was used as a subgrade soil whereas the embankment were built from a
657 typical graded sand. Five loading stages were applied in each test. The following conclusions can be
658 drawn out of the presented results and discussion.

659 **1.** During stage 0 (self-weight of embankment), a slight increase on the pressure in pile caps was
660 noted with increasing the number of reinforcement layers. However, a distinctive difference

occurred in the pressure transferred to the pile caps during the monotonic loading stage in which surface pressure was increased to 31kPa. This could be attributed to the pure arching effect in the case of the unreinforced embankment and the combination of load transfer mechanisms in reinforced embankments.

2. The results suggest that shallow unreinforced embankments perform poorly under the effect of cyclic loadings. The collapse of arching is imminent which could lead to significant transfer of the surface loads to the soft ground. However, it was apparent that regain of strength due to densification of the embankment material and deformation of the soft subgrade soil would lead to partial or full recovery of the arching effect with further stages of cyclic loading.

3. A good degree of improvement in response and performance of piled embankments was noticeable with increasing the number of reinforcement layers. The measured data showed clearly that with increasing number of reinforcement layers, most of the surface load was transferred to the piles irrespective of the cyclic loading stage.

4. The tension force in the reinforcement layers was measured to be at the highest value in the bottom reinforcement layer and reduced with increasing the number of reinforcement layers.

5. Almost 50 % of the surface settlement occurred during the first 100 cycles of cyclic loading. Increasing the number of reinforcement layers led to a remarkable reduction in the measured surface settlement and deformation (e.g. settlement and heave) of the soft subsoil.

LIST OF NOTATIONS

a pile width (m)

d_{10} Diameter of 10% passing (μ)

d_{30} Diameter of 30% passing (μ)

d_{50} Diameter of 50% passing (μ)

d_{60} Diameter of 60% passing (μ)

E Load transfer efficiency (dimensionless)

H Embankment height (m)

s' Clear spacing between piles (m)

SCR Stress Concentration Ratio (dimensionless)

σ_p Measured pressure on piles (Pa)

σ_s Measured pressure on soft subsoil (Pa)

680 **LIST OF ABREVIATIONS**

681

ASMP Applied Surface Mean Pressure

Amp Amplitude

C Clay powder

CS Coarse sand

Freq Frequency

FS Fine sand

LVDT Linear Variable Differential Transducer

PP Polypropylene

682 **REFERENCES**

683 Abusharar, S.W., Zeng, J.J., Chen, B.G.& Yin, J.H. (2009). A simplified method for analysis of appiled
684 embankment reinforced with geosynthetics. *Geotextiles and Geomembranes,* 27, 39-52.
685 Almeida, M.S.S., Ehrlich, M., Spotti, A.P. & Marques, M.E.S. (2007). Embankment supported on piles
686 with biaxial geogrids. *Proceedings of the Institution of Civil Engineers-Geotechnical Engineering*,
687 160(4), 185-192.

688 Ariyarathne, P., Liyanapathirana, D.S. & Leo, C.J. (2013). Effect of geosynthetic creep on reinforced pile-
689 supported embankment systems. *Geosynthetics International*, Vol. 20(6), pp. 421-435.
690 Ariyarathne, P. & Liyanapathirana, D.S. (2014). Significance of geosynthetic reinforcement in
691 embankment construction. *Australian Geomechanics Journal*, 49(3), pp.15-28.
692 Aqoub, K., Mohamed, M. & Sheehan, T. (2018). Analysis of sequential active and passive arching in
693 granular soils. International Journal of Geotechnical Engineering, 12, pp.1-10.
694 Azizi, F. (1999). Applied analyses in geotechnics. CRC Press.
695 Bhasi, A. & Rajagopal, K. (2015). Numerical study of basal reinforced embankments supported on
696 floating/end bearing piles considering pile–soil interaction. *Geotextiles and Geomembranes*,
697 43(6), 524–536.
698 Blanc, M., Rault, G., Thorel, L. & Almeida, M. (2013). Centrifuge investigation of load transfer
699 mechanisms in a granular mattress above a rigid inclusions network. *Geotextiles and*
700 *Geomembranes*, 36, 92–105.
701 Briançon, L. & Simon, B. (2012). Performance of pile-supported embankment over soft soil: full-scale
702 experiment. *Journal of Geotechnical and Geoenvironmental Engineering*, 138(4), 551-561.
703 Briançon, L. & Simon, B. (2017). Pile-supported embankment over soft soil for a high-speed line.
704 *Geosynthetics International*, 1–13
705 British Standards Institution (1999), BS 5930:1999 *Code of practice for site investigations*
706 British Standard (2002), BS EN ISO 14688 - 1:2002 *Geotechnical investigation testing Identification and*
707 *classification of soil, Part 1: Identification and description.*
708 British Standard (2004), BS EN ISO 14688 - 2:2004 *Geotechnical investigation testing Identification and*
709 *classification of soil, Part 2: Principles for a classification of soil.*
710 BS EN ISO 10319:2015 - *Geosynthetics. Wide-width tensile test*, British Standards Institution, London,
711 United Kingdom.

British Standard, BS8006 (1995). *Code of practice for strengthened/reinforced soils and other fills*. British Standards Institution, London.

British Standard, BS8006-1: (2010). *Code of practice for strengthened/reinforced soils and other fills*. British Standards Institution, London.

Chen, Yun-Min, Cao, Wei-Ping & Chen, Ren-Peng. (2008). An experimental investigation of soil arching within basal reinforced and unreinforced piled embankments. *Geotextiles and Geomembranes*, 26(2),164–174.

Collin, J.G., (2004). Column supported embankment design considerations. *52nd Annual Geotechnical Engineering Conference*-.University of Minnesota, Minneapolis, MN. February 27, 2004.

Cui, Z.D., Yuan, Q. & Yang, J.Q. (2018). Laboratory model tests about the sand embankment supported by piles with a cap beam. *Geomechanics and Geoengineering*, 13(1), pp.64-76.

Das, B.M., (2010). Geotechnical engineering handbook. J. Ross Publishing.

Deb, K., & Mohapatra, S.R. (2013). "Analysis of stone column-supported geosynthetic reinforced embankments." *Appl. M ath. Model*., 37(5), 2943–2960.

Elshesheny, A., Mohamed, M. & Sheehan, T. (2018). Buried flexible pipes behaviour in unreinforced and reinforced soils under cyclic loading. *Geosynthetics International*. (Accepted).

Eskişar, T., Otani, J. & Hironaka, J. (2012). Visualization of soil arching on reinforced embankment with rigid pile foundation using X-ray CT. *Geotextiles and Geomembranes*, 32, 44–54.

Fagundes, D.F., Almeida, M.S., Thorel, L. & Blanc, M. (2017). Load transfer mechanism an deformation of reinforced piled embankments. *Geotextiles and Geomembranes*, 45(2), pp.1-10.

Girout, R., Blanc, M., Thorel, L. & Dias, D. (2018). Geosynthetic reinforcement of pile-supported embankments. *Geosynthetics International*,25(1) pp. 37-49.

Guido, V.A., Kneuppel, Sweeney, M.A., (1987). Plate loading test on geogrid reinforced earth slabs. *In: Proceedings Geosynthetics, 87 Conference*, New Orleans, 216–225.

736 Han, J., & Gabr, M.A. (2002). Numerical analysis of geosynthetic-reinforced and pile-supported earth
737 platforms over soft soil. *Journal of geotechnical and geoenvironmental engineering*, 128(1), 44-
738 53.
739 Han, G.X., Gong, Q.M. & Zhou, S.H. (2015). Soil arching in a piled embankment under dynamic load.
740 *International Journal of Geomechanics*, 15(6), pp.1-7.
741 Heitz, C. (2006). Bodengewölbe unter ruhender und nichtruhender Belastung bei Berücksichtigung von
742 Bewehrungseinlagen aus Geogittern. *Schriftenreihe Geotechnik*, University of Kassel, Issue 19
743 Heitz, C., Luking, J. & Kempfert, H-G. (2008). Geosynthetic reinforced and pile supported embankments
744 under static and cyclic Loading. In: *Proceedings of the 4th European Geosynthetics. Conf Euro-*
745 *Geo4*, Edinburgh (UK), paper no 215,pp.1-8.
746 Hewlett, W.J. & Randolph, M.F. (1988). Analysis of piled embankment. *Ground Engineering. 21:12-18.*
747 Houda, M., Jenck, O. & Emeriault, F. (2016). Physical evidence of the effect of vertical cyclic loading on
748 soil improvement by rigid piles: a small-scale laboratory experiment using Digital Image
749 Correlation. *Acta Geotechnica*, 11(2), pp.325-346.
750 Kempton, G., Russell, D., Pierpoint, N.D. & Jones, C.J.F.P. (1998). Two-and three-dimensional numerical
751 analysis of the performance of piled embankments. *In Proceedings, 6th International Conference*
752 *on Geosynthetics.* Atlanta,GA*,* (Vol. 2, pp. 767-772).
753 Kempfert, H.G., Zaeske, D. & Alexiew, D. (1999). Interactions in reinforced bearing layers over partial
754 supported underground. In: *Geotechnical Engineering for Transportation Infrastructure*,
755 Balkema, Rotterdam, The Netherlands, 1527–1532.
756 Kempfert, H.G., Göbel, C., Alexiew, D., & Heitz, C. (2004). German recommendations for reinforced
757 embankments on pile-similar elements. In: *EuroGeo3-3rd European geosynthetics conference,*
758 *Geotech Eng with Geosynthetics*, Munich, Germany,pp. 279–284.

759 Kongkitkul, W., Hirakawa, D., Tatsuoka, F. & Uchimura, T. (2004). Viscous deformation of geosynthetic
760 reinforcement under cyclic loading conditions and its model simulation. *Geosynthetics*
761 *International,* 11(2), pp.73-99.
762 Jenck, O., Dias, & D. Kastner, R. (2009). Three-dimensional numerical modeling of a piled embankment.
763 *International Journal of Geomechanics*, 9(3), 102-112.
764 Latha, M.G. & Murthy, V.S., (2006). Investigations on sand reinforced with different geosynthetics.
765 *Geotechnical Testing Journal*, 29(6), pp.474-481.
766 Lehn, J., Moormann, C. & Aschrafi, J. (2016). Numerical Investigations on the Load Distribution over the
767 Geogrid of a Basal Reinforced Piled Embankment under Cyclic Loading. *Procedia Engineering*,
768 143, pp.435-444.
769 Liu, H. L., Ng, C.W. & Fei, K. (2007). Performance of a geogrid-reinforced and pile-supported highway
770 embankment over soft clay: case study. *Journal of Geotechnical and Geoenvironmental*
771 *Engineering*, 133(12), 1483-1493.
772 Love, J. & Milligan, G. (2003). Design methods for basally reinforced pile-supported embankments over
773 soft ground, *Ground Engineering*, 36(3).
774 Low, B.K., Tang, S.K. & Choa, V. (1994). Arching in piled embankments. *Journal of Geotechnical*
775 *Engineering,* 120(11):1917–1938.
776 Jones, C.J.F.P, Lawson, C.R., Ayres, D.J., (1990). Geotextile reinforced piled embankments. In:
777 *Proceedings of the Fourth International Conference on Geotextiles: Geomembranes and Related*
778 *Products,* Balkema,Rotterdam, The Netherlands, pp.155–160.
779 Magnan, J-P. (1994). Methods to reduce the settlement of embankments on soft clay: *Vertical and*
780 *horizontal deformations of foundations and embankments*. ASCE, 1(40):77–91.

781 Mohamed, M. H. (2010). Two dimensional experimental study for the behaviour of surface footings on
782 unreinforced and reinforced sand beds overlying soft pockets. *Geotextiles and Geomembranes*,
783 28, No. 6, 589–596.
784 Nunez, M. A., Briançon, L. & Dias, D. (2013). Analyses of a pile-supported embankment over soft clay:
785 Full-scale experiment, analytical and numerical approaches. *Engineering Geology*, 153, 53-67.
786 Oh, Y.I. & Shin, E.C. (2007). Reinforced and arching effect of geogrid-reinforced and pile-supported
787 embankment on marine soft ground. *Marine Georesources and Geotechnology*, 25, 97-118.
788 Rowe, R.K. & Li, A.L.,(1999). Reinforced embankments over soft foundations under undrained and
789 partially drained conditions. *Geotextiles and Geomembranes*, 17(3), pp.129-146.
790 Russell, D. & Pierpoint, N. (1997). An assessment of design methods for piled embankments. *Ground*
791 *Engineering,* 30 (11), 39–44.
792 Russell, D., Naughton, P.J. & Kempton, G. (2003). 'A new design procedure for pile embankments'*, In:*
793 *Proceedings of the 56th Canadian Geotechnical Conference and 2003 NAGS Conference, CGS*
794 Winnipeg, MB. (Vol. 1, pp. 858-865).
795 Shen, S.L., Chai, J.C., Hong, Z.S. & Cai, F.X. (2005). Analysis of field performance of embankments on soft
796 clay deposit with and without PVD-improvement. *Geotextiles and Geomembranes,* 23 (6), 463–
797 485.
798 Stewart, M.E. & Filz, G.M. (2005). Influence of clay compressibility on geosynthetic loads in bridging
799 layers for column-supported embankments. In *Contemporary issues in foundation engineering.*
800 ASCE (pp. 1-14).
801 Terzaghi, K. (1943). 'Theoretical Soil Mechanics', John Wiley and Sons, New York.
802 Van Eekelen, S.J.M. & Nancey, A., Bezuijen, A., (2012). Influence of fill material and type of geosynthetic
803 reinforcement in a piled embankment, model experiments. In: *Proceedings of EuroGeo5,*
804 *Valencia,* Spain. (Vol. 5, pp. 167-171).

Van Eekelen, S.J.M. (2015). Basal Reinforced Piled Embankments. Experiments, field studies and the development and validation of a new analytical design model (Doctoral dissertation, PhD thesis, Delft University of Technology).

Van Eekelen, S. J. M., Bezuijen, A., & van Tol, A. F. (2015). Validation of analytical models for the design of basal reinforced piled embankments. *Geotextiles and Geomembranes*, 43(1), 56–81

Van Eekelen S.J.M. & Bezuijen A. (2012). Model experiments on geosynthetic reinforced piled embankments, 3D test series. *In 2nd European conference on physical modelling in geotechnics* (EUROFUGE-2012). Delft, The Netherlands. (pp. 1-10).

Van Eekelen, S.J.M., Bezuijen, A., Lodder, H. J. & van Tol, A. F.(2012a). "Model experiments on piled embankments. Part I." *Geotextiles and Geomembranes*, 32(3), 69–81.

Van Eekelen, S.J.M., Bezuijen, A., Lodder, H. J. & van Tol, A. F. (2012b). "Model experiments on piled embankments. Part II." *Geotextiles and Geomembranes*, 32(3), 82–94.

Van Eekelen, S.J.M., Bezuijen, A. & Van Tol, A.F. (2011). Analysis and modification of the British Standard BS8006 for the design of piled embankments. *Geotextiles and Geomembranes,29, 345–359.*

Van Eekelen, S.J.M., Jansen, H.L., Van Duijnen, P.G., De Kant, M., Van Dalen, J.H., Brugman, M.H.A., van der Stoel, A. & Peters, M.G.J.M. (2010). The Dutch design guideline for piled embankments. In *9th international conference on geosynthetics, geosynthetics for a challenging world,* 23-27 May (2010), Guaruja, Brasil. IGS. (pp. 1911-1916).

Van Eekelen, S.J.M., Bezuijen, A. & van Tol, A.F., (2013). An analytical model for arching in piled embankments. *Geotextiles and Geomembranes*, 39, pp.78-102.

Van Eekelen, S.J.M. (2016). The 2016-update of the Dutch Design Guideline for Basal Reinforced Piled Embankments. *Procedia engineering*, 143, pp.582-589.

827 Villard, P., Le Hello, B., Nancey, A., Chew, S.H. & Loke, K.H. (2004), March. Use of high strength
828 geotextiles over piles results from a full-scale test'. In *Proceedings of the 3nd European*
829 *Geosynthetics Conference, Munich, Germany* (Vol. 1, pp. 295-29).
830 Villard, P. & Giraud, H. (1998). Three-dimensional modelling of the behaviour of geotextile sheets as
831 membranes. *Textile Research Journal,* 68(11), pp.797-806.
832 Wang, K.Y., Zhuang, Y., Liu, H. & Miao, Y. (2018). Soil arching in highway piled embankments subjected
833 to moving shakedown limit loads. *European Journal of Environmental and Civil Engineering*, 1-
834 15.
835 Zaeske, D. (2001). Zur Wirkungsweise von unbewehrten und bewehrten mineralischenTragschichten
836 über pfahlartigen Gründungselementen. *Schriftenreihe Geotechnik*, Uni Kassel, Heft 10, February
837 2001 (in German).
838 Zanzinger, H., Hangen, H. & Alexiew, D. (2010). Fatigue behaviour of a PET-Geogrid under cyclic loading.
839 *Geotextiles and Geomembranes*, 28(3), 251-261.
840 Zhang, M.X., Javadi, A.A. & Min, X. (2006). Triaxial tests of sand reinforced with 3D inclusions.
841 *Geotextiles and Geomembranes*, 24(4), pp.201-209.
842 Zhao, L.S., Zhou, W.H. & Yuen, K.V. (2017). A simplified axisymmetric model for column supported
843 embankment systems. *Computers and Geotechnics*, 92, pp.96-107.
844 Zhuang, Y., Wang, K.Y. & Liu, H.L. (2014). A simplified model to analyse the reinforced piled
845 embankments, *Geotextiles and Geomembranes*, Volume 42, Issue 2, April 2014, 154-165.
846 Zhuang, Y. & Li, S. (2015). Three-dimensional finite element analysis of arching in a piled embankment
847 under traffic loading. *Arabian Journal of Geosciences*, 8(10), pp.7751-7762.
848 Zhuang, Y. & Wang, K.Y. (2018). Finite element analysis on the dynamic behaviour of soil arching effect
849 in piled embankment. *Transportation Geotechnics*, 14, pp.8-21.
850

851

852 **List of Tables:**

853 **Table 1.** Scaling rules for experiment against Prototype

Parameter	Dimension	Scale ratio
Length	m	1: x
Area	m^2	1: x^2
Stress	kPa	1:1
Force	kN	1: x^2
Tensile strength of reinforcement	kN/m	1: x
Deformation and distances	m/m	1:1

854

855

856 **Table 2.** Scaling applied in this study

Parameters	Laboratory	Prototype
Testing tank dimensions, m	1.5 x 1.0	6.0 x 4.0
Centre-to-centre pile spacing, m	0.5	2.0
Pile cap width, m	0.1	0.40
Embankment height, m	0.2	0.80
Tensile strength of reinforcement, kN/m’	9.0	36.0
Surface maximum pressure due to traffic load, kPa	53-98	53-98
Pressure due to self-weight of embankment, kPa	3.36	13.44

857

858

859

860 **Table 3.** Properties of sand fill used in this study

Property	Measured value
d_{10}, μm	170
d_{30}, μm	350
d_{50}, μm	600
d_{60}, μm	850
Uniformity coefficient (C_u)	5
Coefficient of curvature (C_c)	0.85
Maximum dry unit weight, kN/m^3	17.96
Optimum water content, %	10.30
Specific gravity	2.65
Angle of friction, degree	38^O
Angle of friction between sand and reinforcement layer, degree	26^O

861

862

863

Table 4. Properties of used soft subsoil in this study

Property	Measured value
Dry unit weight, kN/m^3	15.95
Moisture content, %	22.0
Liquid limit, %	28.0
Plastic limit, %	20.2
Undrained cohesion, kPa	13
Angle of friction, degree	0
Elastic modulus, kPa	425

List of Figures

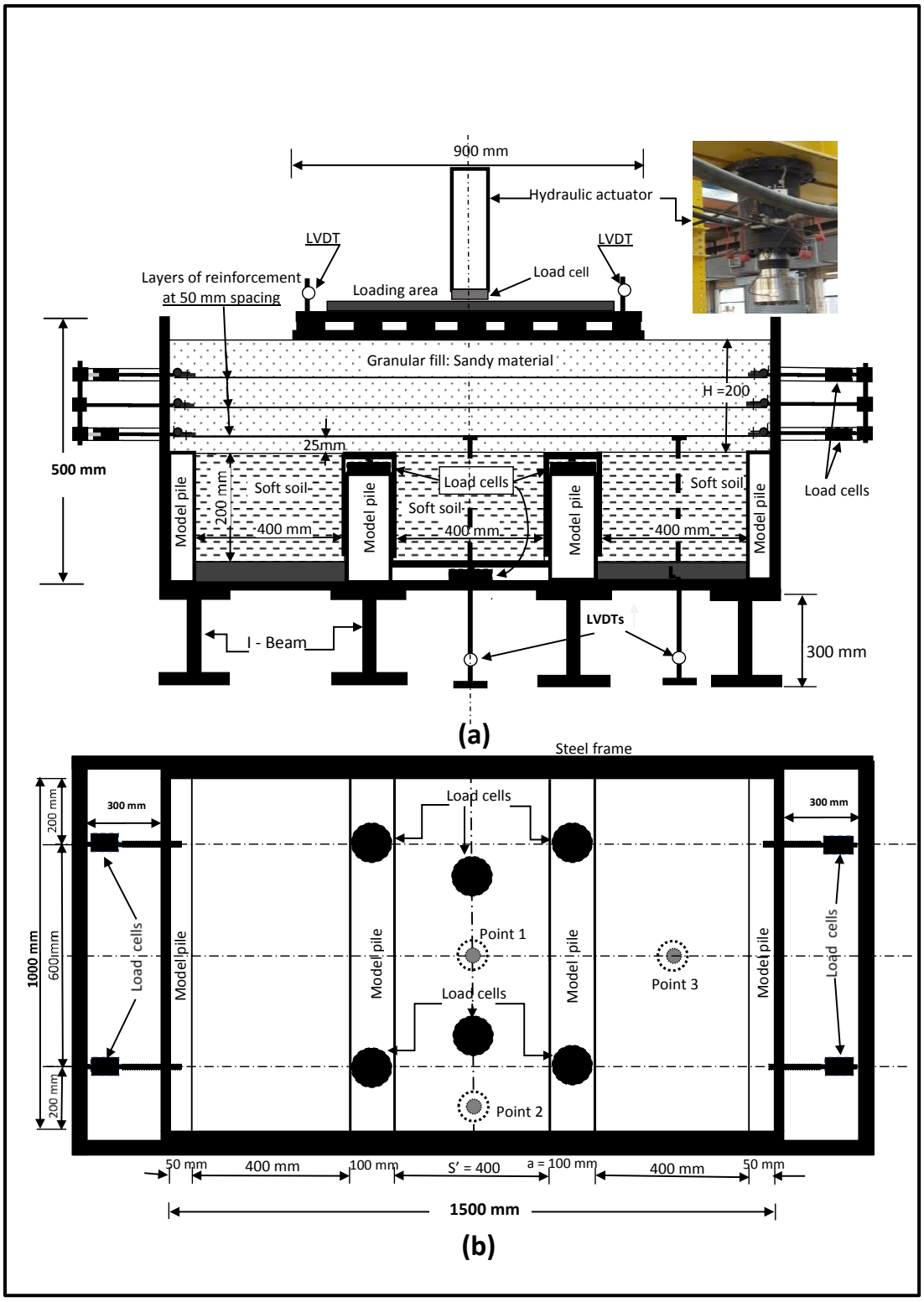

880

881 **Figure 1.** Schematic drawing of the testing rig (a) vertical cross section (b) Plan view

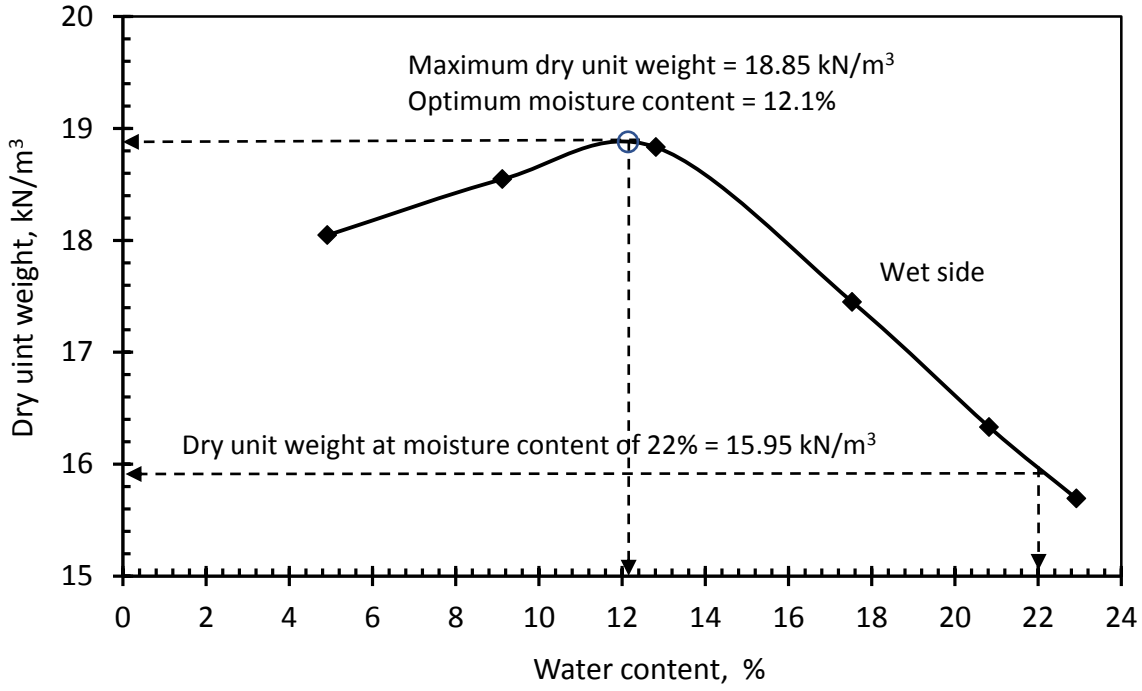

882

883 **Figure 2.** Compaction curve of soft subsoil

884

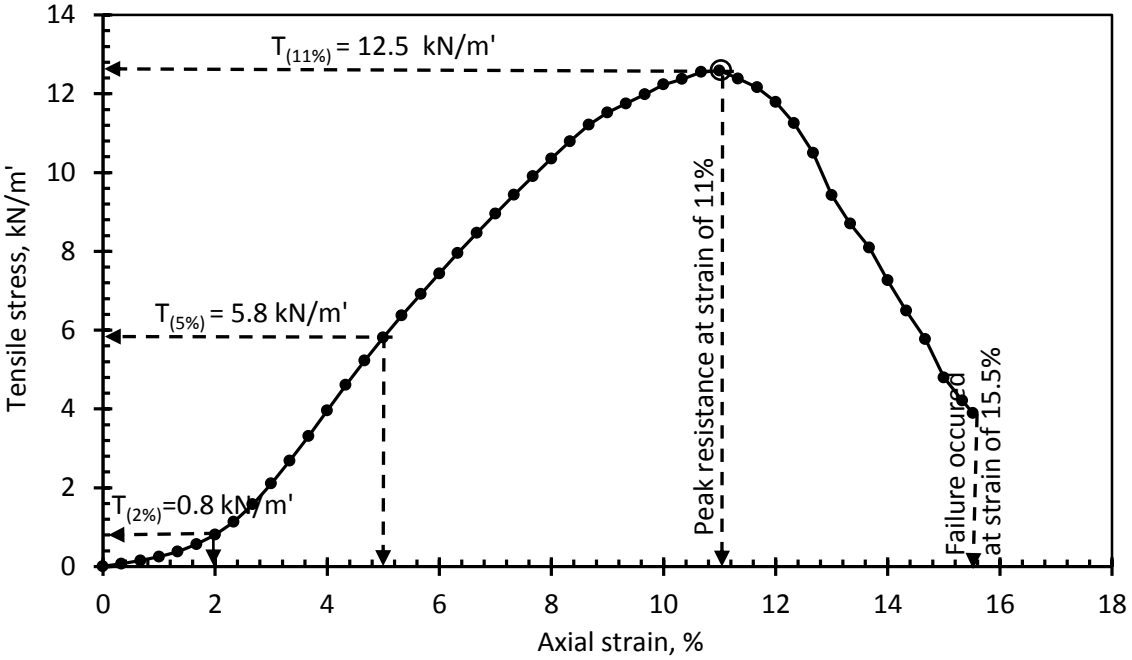

Figure 3. Tensile stress – strain relationship for the used woven PP geotextile reinforcement material

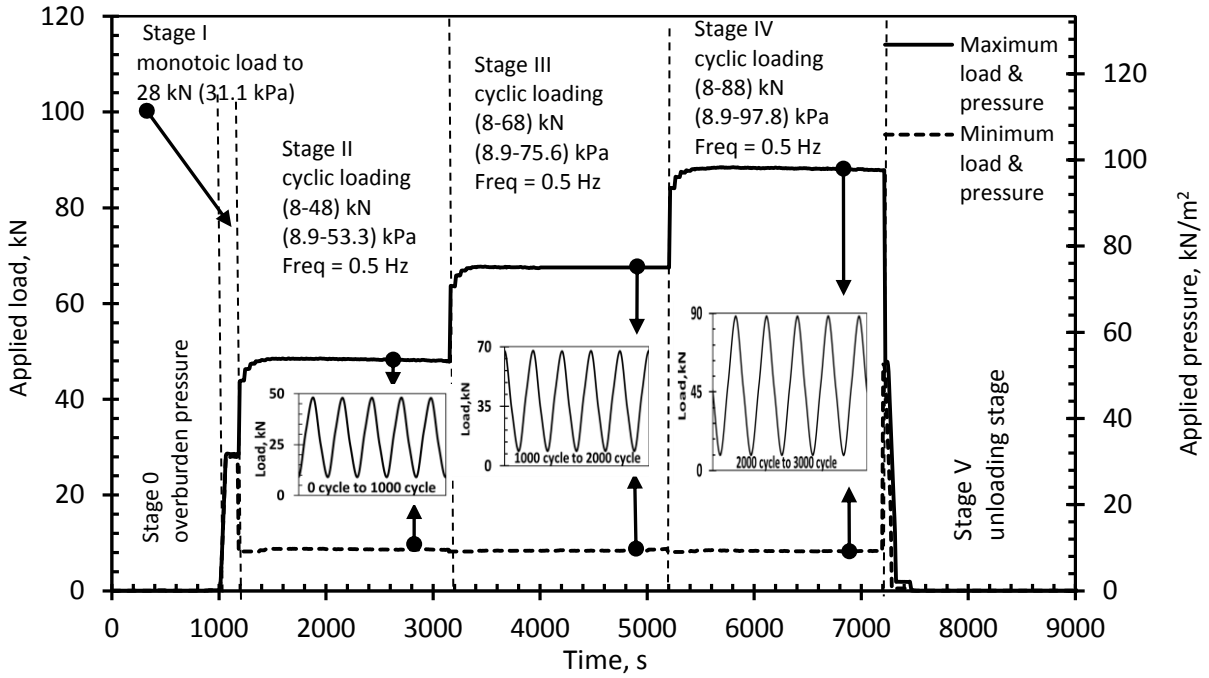

Figure 4. Different stages of maximum and minimum monotonic and cyclic loadings

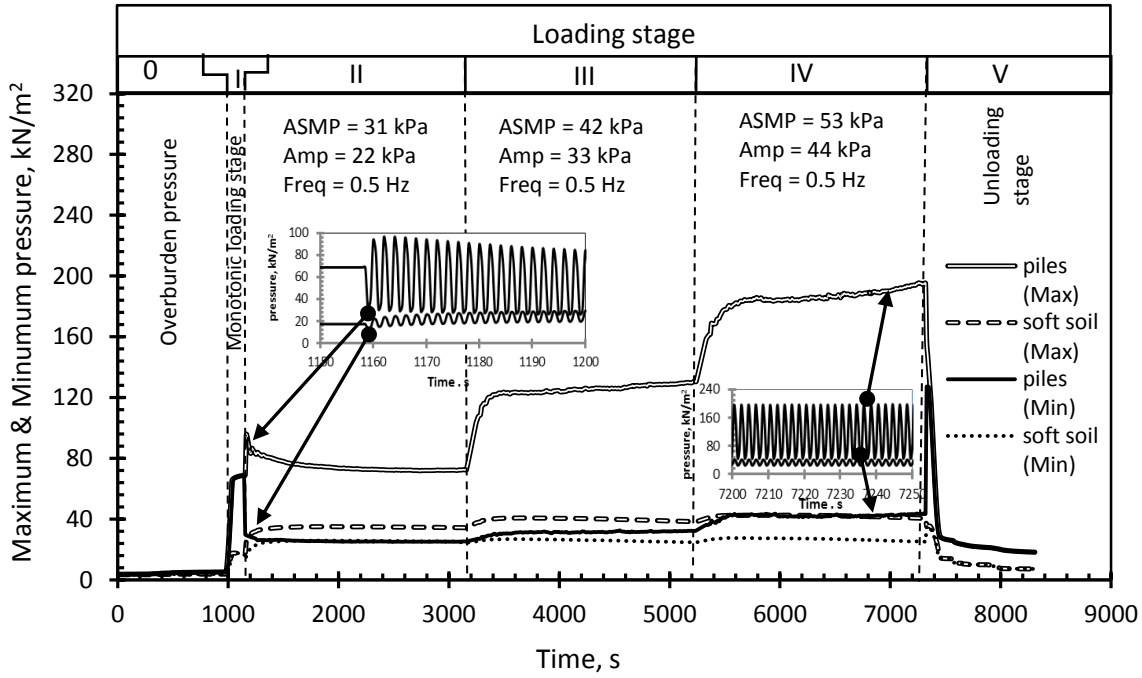

900

901 **Figure 5**. Maximum and Minimum pressure on pile caps and soft subsoil for unreinforced embankment.

902 where; ASMP = Applied Surface Mean Pressure, Amp = Amplitude and Freq = Frequency.

903

904

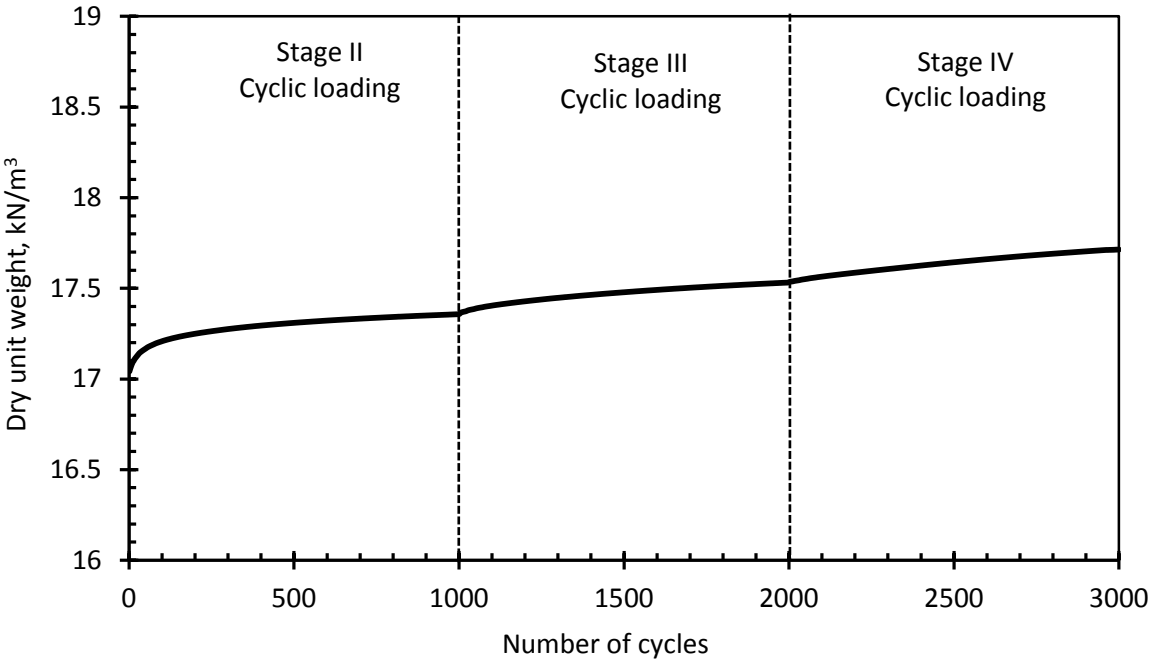

Figure 6. Estimated dry unit weights of unreinforced embankment during cyclic load

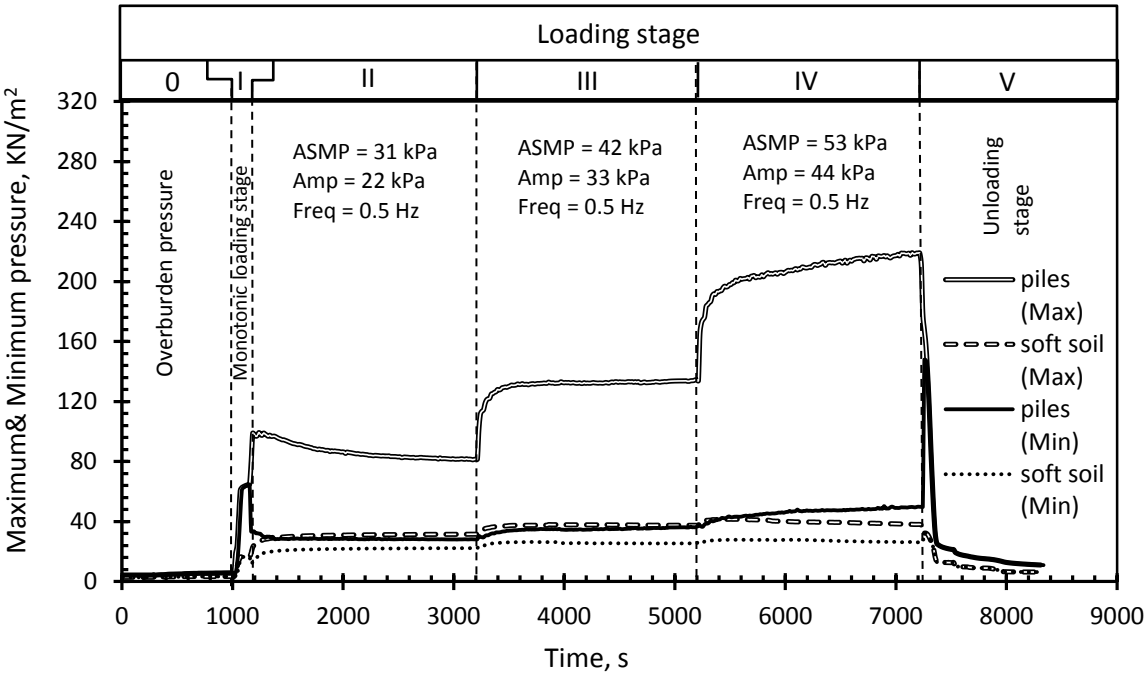

919

920 **Figure 7.** Maximum and Minimum pressure on pile caps and soft subsoil for one layer reinforced

921 embankment

922

923

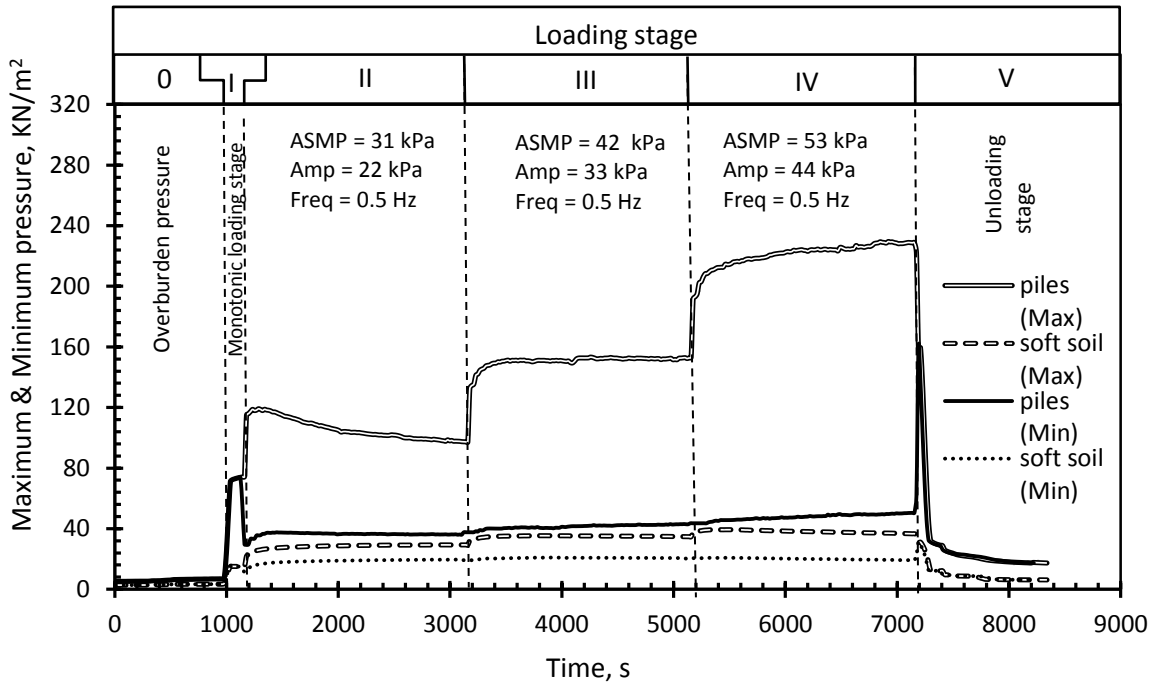

924

925 **Figure 8.** Maximum and minimum pressure on pile caps and soft subsoil for two layers reinforced

926 embankment

927

928

929

930

931

932

933

934

935

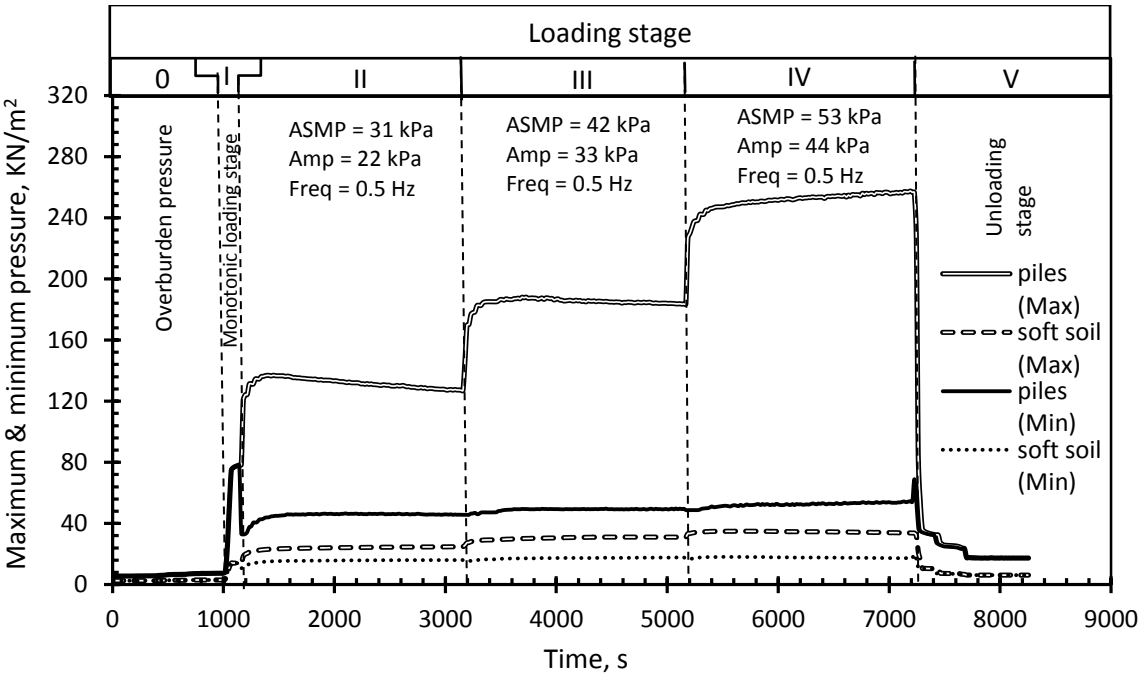

936

937 **Figure 9.** Maximum and minimum pressure on pile caps and soft subsoil for three layers reinforced

938 embankment

939

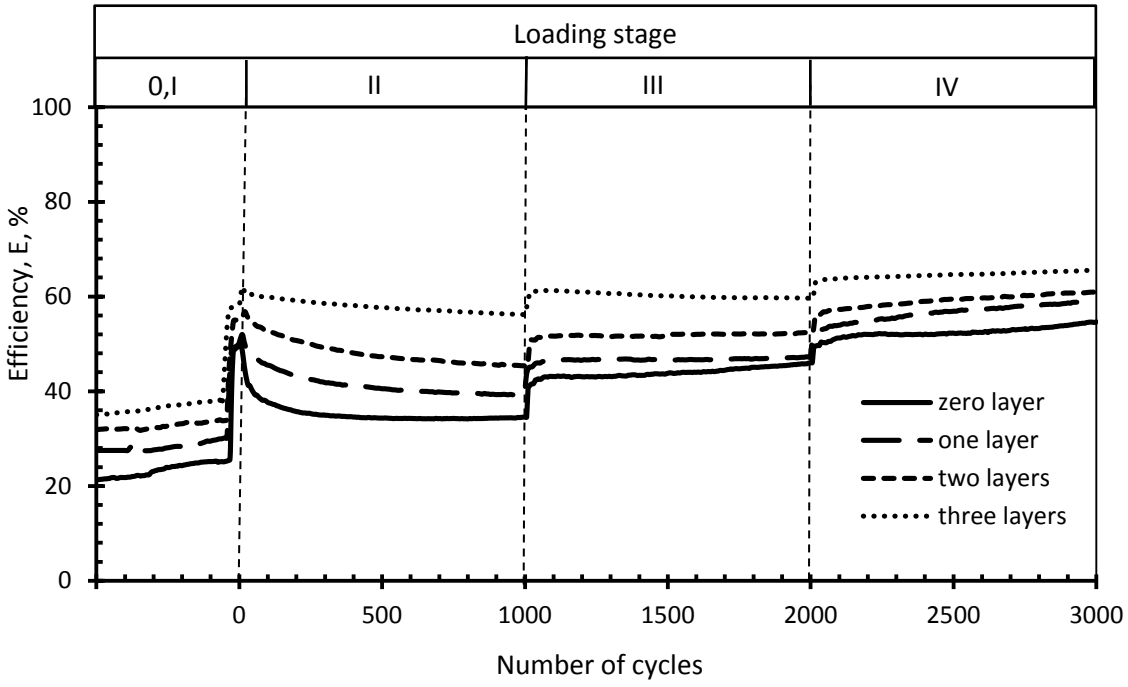

940
941 **Figure 10.** Efficiency of unreinforced and reinforced embankment versus number of cycles.

942

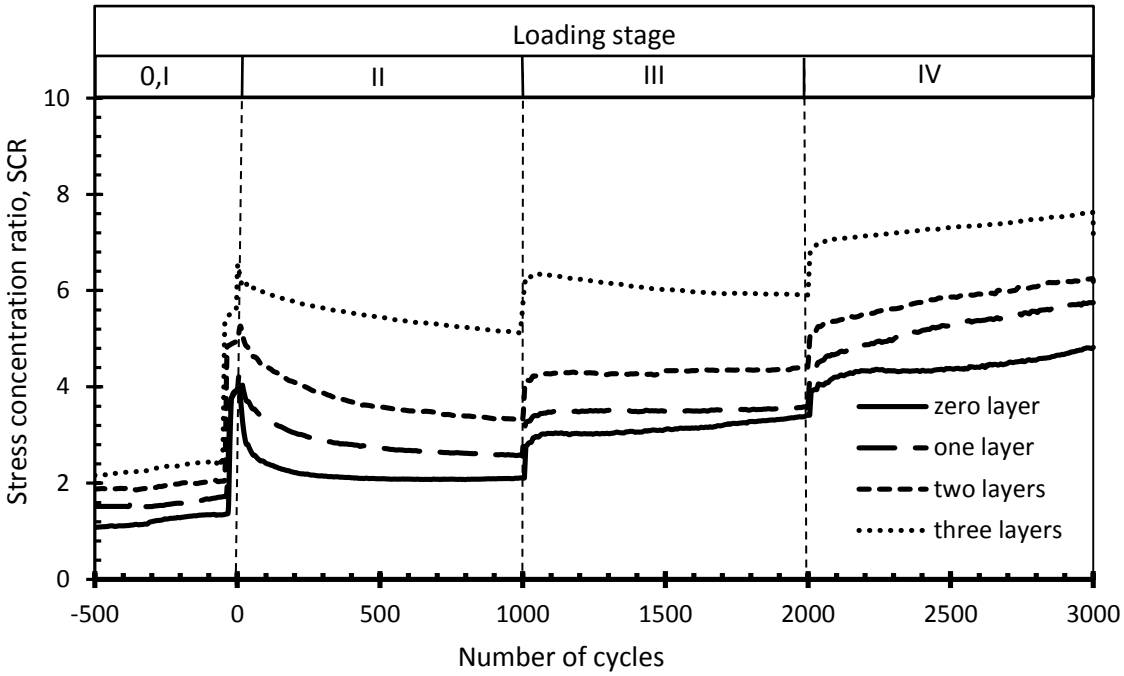

943

944 **Figure 11. S**tress concentration ratio of unreinforced and reinforced embankment versus number of

945 cycles.

946
947

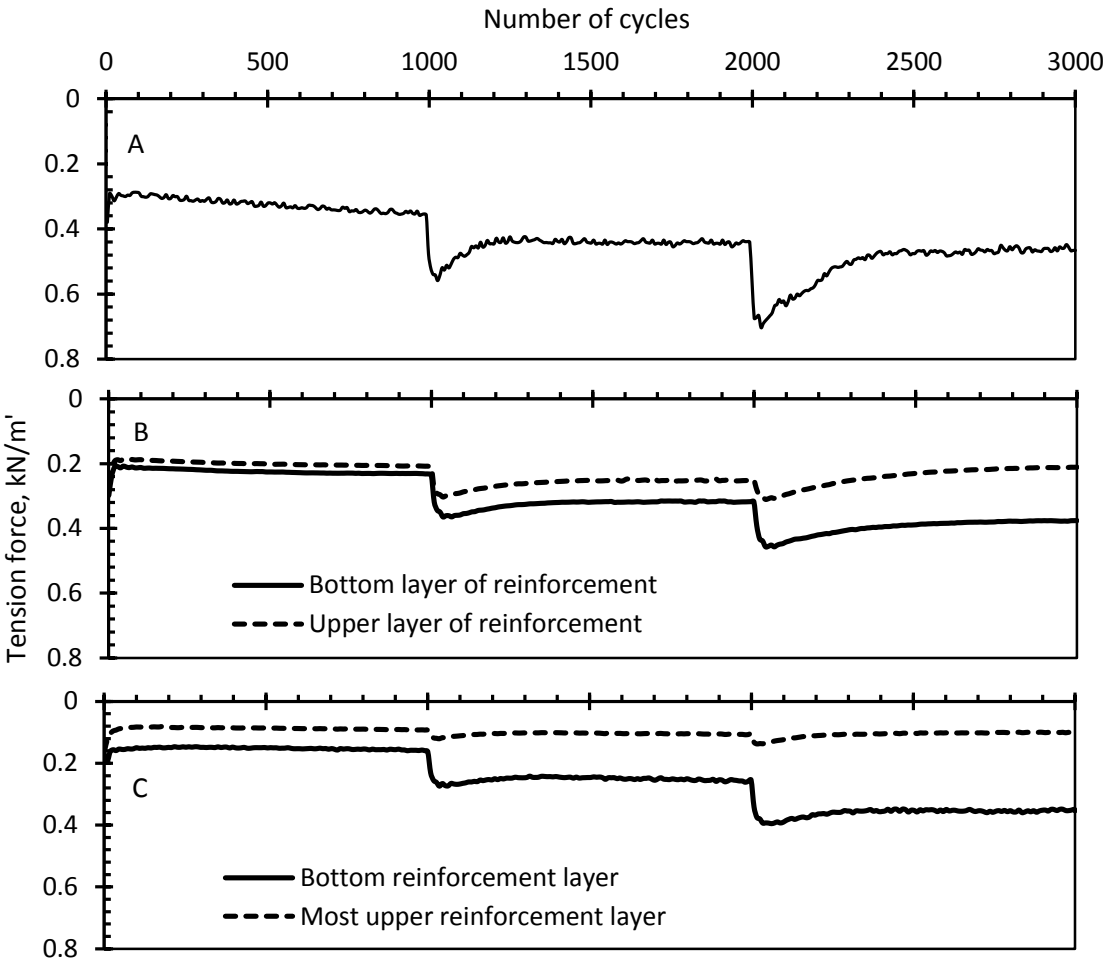

948

949

950

951 **Figure 12.** Measured tension force in reinforcement layers on embankments with; A) one layer of

952 reinforcement, B) two layers of reinforcement and C) three layers of reinforcement

953

954

955

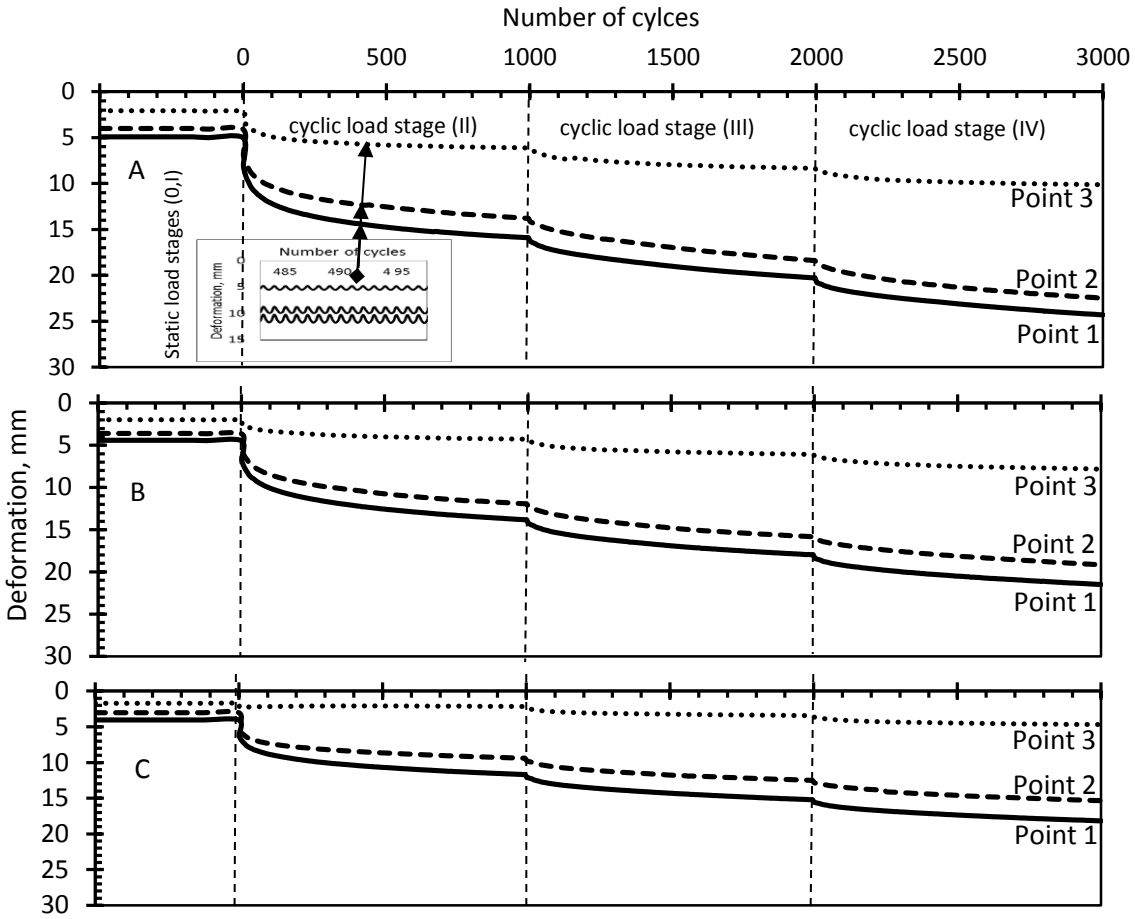

956

957

958

959

960 **Figure13.** Maximum deformations in the bottom reinforcement layer versus number of cycles for ; A)

961 one layer of reinforcement, B) two layers of reinforcement and C) three layers of reinforcement

962

963

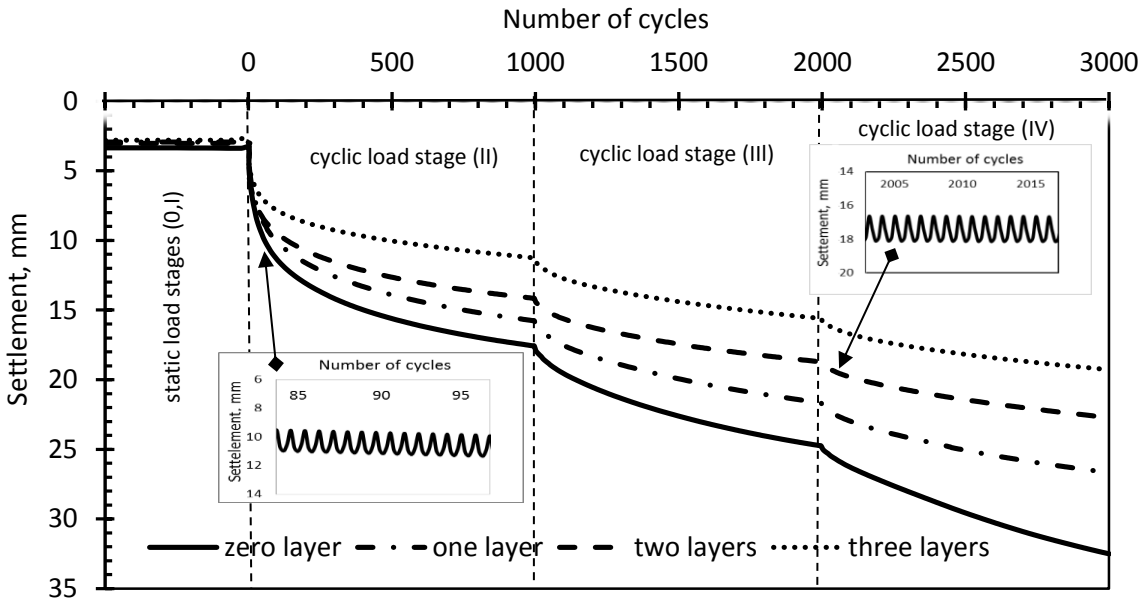

964

965 **Figure 14.** Maximum settlement of loading plate versus number of cycles

966

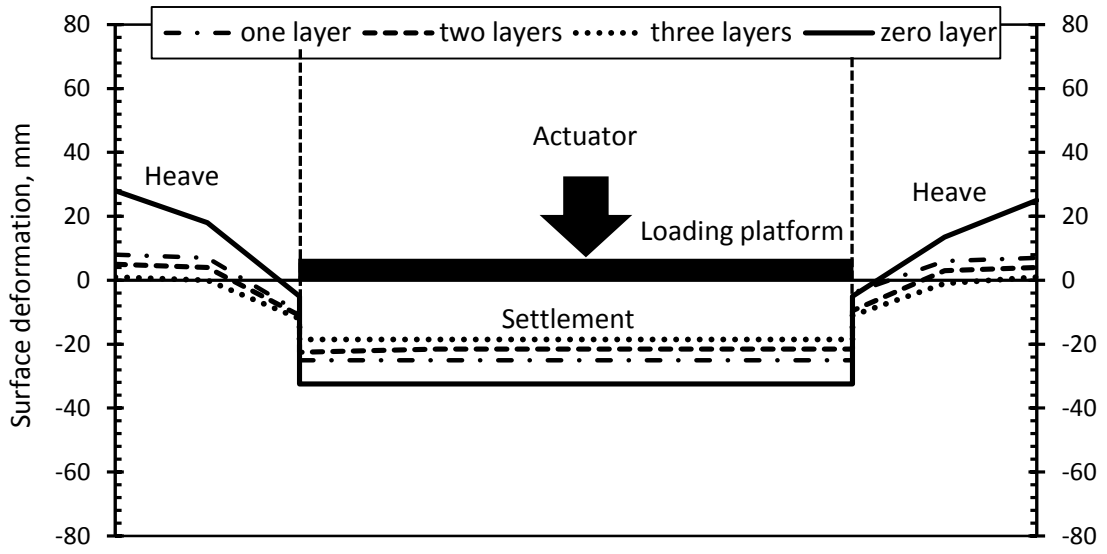

Figure 15. Soil surface settlement after removing the applied loads versus the box test distance.

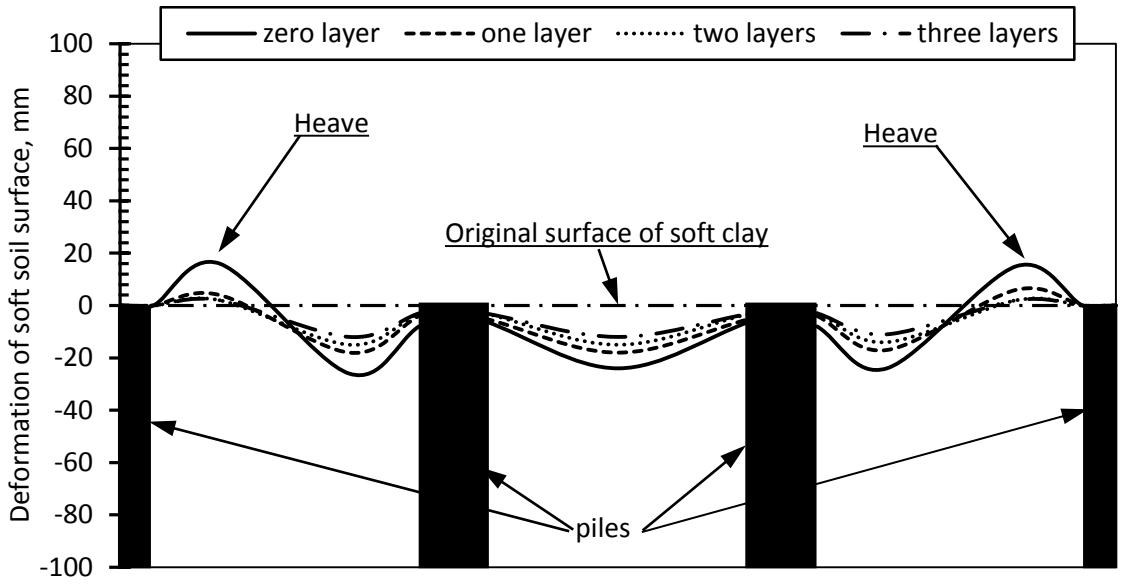

984

985 **Figure 16.** Deformed surface of soft subsoil after completion of test

986

987

988